Dalton Transactions

PAPER

View Article Online
View Journal | View Issue

Cite this: *Dalton Trans.*, 2015, **44**, 9071

Strong effect of copper(II) coordination on antiproliferative activity of thiosemicarbazone–piperazine and thiosemicarbazone–morpholine hybrids†

Felix Bacher,[a] Orsolya Dömötör,[b] Anastasia Chugunova,[a] Nóra V. Nagy,[c] Lana Filipović,[d] Siniša Radulović,[d] Éva A. Enyedy*[e] and Vladimir B. Arion*[a]

In this study, 2-formylpyridine thiosemicarbazones and three different heterocyclic pharmacophores were combined to prepare thiosemicarbazone–piperazine mPip-FTSC (**HL^1**) and mPip-dm-FTSC (**HL^2**), thiosemicarbazone–morpholine Morph-FTSC (**HL^3**) and Morph-dm-FTSC (**HL^4**), thiosemicarbazone–methylpyrrole-2-carboxylate hybrids mPyrr-FTSC (**HL^5**) and mPyrr-dm-FTSC (**HL^6**) as well as their copper(II) complexes [CuCl(mPipH-FTSC-H)]Cl (**1** + H)Cl, [CuCl(mPipH-dm-FTSC-H)]Cl (**2** + H)Cl, [CuCl(Morph-FTSC-H)] (**3**), [CuCl(Morph-dm-FTSC-H)] (**4**), [CuCl(mPyrr-FTSC-H)(H_2O)] (**5**) and [CuCl(mPyrr-dm-FTSC-H)(H_2O)] (**6**). The substances were characterized by elemental analysis, one- and two-dimensional NMR spectroscopy (**HL^1–HL^6**), ESI mass spectrometry, IR and UV–vis spectroscopy and single crystal X-ray diffraction (**1–5**). All compounds were prepared in an effort to generate potential antitumor agents with an improved therapeutic index. In addition, the effect of structural alterations with organic hybrids on aqueous solubility and copper(II) coordination ability was investigated. Complexation of ligands **HL^2** and **HL^4** with copper(II) was studied in aqueous solution by pH-potentiometry, UV–vis spectrophotometry and EPR spectroscopy. Proton dissociation processes of **HL^2** and **HL^4** were also characterized in detail and microscopic constants for the *Z*/*E* isomers were determined. While the hybrids **HL^5**, **HL^6** and their copper(II) complexes **5** and **6** proved to be insoluble in aqueous solution, precluding antiproliferative activity studies, the thiosemicarbazone–piperazine and thiosemicarbazone–morpholine hybrids **HL^1–HL^4**, as well as copper(II) complexes **1–4** were soluble in water enabling cytotoxicity assays. Interestingly, the metal-free hybrids showed very low or even a lack of cytotoxicity (IC_{50} values > 300 μM) in two human cancer cell lines HeLa (cervical carcinoma) and A549 (alveolar basal adenocarcinoma), whereas their copper(II) complexes were cytotoxic showing IC_{50} values from 25.5 to 65.1 μM and 42.8 to 208.0 μM, respectively in the same human cancer cell lines after 48 h of incubation. However, the most sensitive for **HL^4** and complexes **1–4** proved to be the human cancer cell line LS174 (colon carcinoma) as indicated by the calculated IC_{50} values varying from 13.1 to 17.5 μM.

Received 18th March 2015,
Accepted 10th April 2015

DOI: 10.1039/c5dt01076d

www.rsc.org/dalton

[a]*University of Vienna, Faculty of Chemistry, Institute of Inorganic Chemistry, Währinger Strasse 42, A-1090 Vienna, Austria. E-mail: vladimir.arion@univie.ac.at*
[b]*MTA-SZTE Bioinorganic Chemistry Research Group, University of Szeged, Dóm tér 7, H-6720 Szeged, Hungary*
[c]*Institute of Organic Chemistry, Research Centre for Natural Sciences, Hungarian Academy of Sciences, Magyar Tudósok körútja 2, H-1117 Budapest, Hungary*
[d]*Institute for Oncology and Radiology of Serbia, Pasterova 14, 11000 Belgrade, Serbia*
[e]*Department of Inorganic and Analytical Chemistry, University of Szeged, Dóm tér 7, H-6720 Szeged, Hungary. E-mail: enyedy@chem.u-szeged.hu*

†Electronic supplementary information (ESI) available: NMR numbering scheme for **HL^1–HL^6** (Scheme S1), synthesis scheme for **HL^1–HL^6** (Scheme S2), deprotonation steps of **HL^2** (Scheme S3), part of the crystal structure of **1** showing complex pairing *via* intermolecular hydrogen bonding interactions (Fig. S1), pH-dependence of the chemical shifts of various protons of **HL^4** (Fig. S2), low- (A) and high-field (B) regions of the ^{1}H NMR spectra **HL^2** at different pH values (Fig. S3), pH-dependence of the chemical shifts of various protons of **HL^2** in the low- (A) and in the high-field (B) regions (Fig. S4), pH-dependence of the molar fraction of the *E* and *Z* isomers of **HL^2** (Fig. S5), 3-dimensional fluorescence spectra of **HL^2** and **HL^4** (Fig. S6), experimental and simulated solution EPR spectra recorded for the copper(II) – **HL^4** system at 1 : 1 (A) and 1 : 2 (B) metal-to-ligand ratio (Fig. S7), calculated component EPR spectra obtained for copper(II) complexes of **HL^2** and **HL^4** in frozen solution (Fig. S8), UV–vis spectra of $[Cu(EDTA)]^{2-}$ in the presence of **HL^2** (Fig. S9), UV–vis spectra of the copper(II) – **HL^2** and **HL^4** systems at 1 : 1 metal-to-ligand ratio (Fig. S10). CCDC 1052906–1052910. For ESI and crystallographic data in CIF or other electronic format see DOI: 10.1039/c5dt01076d

Introduction

Thiosemicarbazones (TSCs) are known as potent metal chelators with high affinity for first row transition metals.[1,2] TSCs and their metal complexes possess a variety of biological activities, such as antifungal, antiviral, antibacterial, antimalarial and anticancer.[3–8] The anticancer activity of α-N-heterocyclic TSCs (HCTs) has been known since the 1950s when 2-formylpyridine thiosemicarbazone (FTSC) showed antileukemic activity in a mice model.[9] To date, the best-studied HCT is 3-aminopyridine-2-carboxaldehyde thiosemicarbazone (3-AP or Triapine). Several clinical phase I and II trials revealed that Triapine is ineffective against a variety of solid tumors but very promising against hematologic malignancies such as leukemia.[10–18] The outcome of a recent clinical phase II study including 37 patients with aggressive myeloproliferative neoplasms, with a response rate of 49% and complete remission in 24% of all patients, has recently been reported.[19] Ribonucleotide reductase (RNR),[20,21] an enzyme catalyzing the reduction of ribonucleotides to the corresponding 2′-deoxyribonucleotides, which is the rate determining step in DNA synthesis,[22] and topoisomerase IIα (Topo IIα), an enzyme that controls the DNA topology during cell division by introducing temporary double strand breaks have been considered as possible targets for this class of compounds.[23–26] New insights into the mechanism of action for RNR inhibiting HCTs and especially Triapine were recently reported.[27–30] The enzymes ATP binding pocket was suggested as major target for Topo IIα inhibiting HCTs.[31] The reaction of copper(II) with HCTs leading to square-planar complexes markedly enhances the Topo IIα inhibition rate.[32]

2-Acetylpyridine thiosemicarbazones possess very high cytotoxicity in human cancer cell lines with IC_{50} values in the nanomolar concentration range and the ability to destroy the tyrosyl radical of the mammalian RNR R2 protein under the slightly reducing conditions typical for tumors.[33,34] However, high general toxicity and, consequently, the low therapeutic index along with low aqueous solubility for these and other related thiosemicarbazones prompted us to design hybrid systems, based on thiosemicarbazones and other pharmacophores. Recently, we prepared proline-TSC hybrids (3-methyl-(*S*)-pyrrolidine-2-carboxylate-2-formylpyridine thiosemicarbazone (L-Pro-FTSC) and 3-methyl-(*R*)-pyrrolidine-2-carboxylate-2-formylpyridine thiosemicarbazone (D-Pro-FTSC)) and their copper(II) complexes.[35] These new compounds are highly water soluble but exhibit very low cytotoxicity, most probably because of their very low lipophilicity. We decided to extend our work and use other pharmacophoric groups for attachment at the 6-position of the TSCs pyridine ring, in order to increase the lipophilicity and modulate the antiproliferative activity. We attached the six-membered rings methylpiperazine and morpholine as well as methylpyrrole-2-carboxylate containing a five-membered planar heterocycle. It is well-known that the attachment of a piperazine moiety on a hydrophobic scaffold has a favourable effect on its water solubility,[36–39] moreover the piperazine heterocycle is found in a broad variety of biologically active compounds, some of which are currently used in clinical therapy.[40–49] Biologically active metal-based compounds containing a piperazine ring have also been reported.[50–54] Morpholine is another well-known water-solubilizing unit incorporated in structures of biologically active compounds, showing often favorable pharmacologic effects.[55–57] In particular, a morpholine moiety is also present in the approved anticancer drugs Gefitinib (against certain breast, lung and other cancers) and Carfilzomib (against multiple myeloma).[58,59] A series of TSCs with different substituents at position 4 of the pyridine ring was tested on mice bearing sarcoma 180 ascites cells. Intriguingly, the 4-morpholino-2-formylpyridine thiosemicarbazone was the most effective compound, increasing the average survival time of tumor bearing mice from 13.8 to 38 days.[60] The methylpyrrole-2-carboxylate ring was chosen as third possible option since it resembles proline.

Herein, we report the synthesis of six new organic compounds, namely **HL$^{1-6}$**, representing three types of potential hybrid ligands for transition metals, as well as six copper(II) complexes all shown in Chart 1. The compounds were charac-

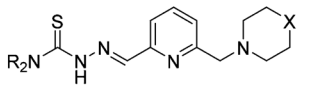

R = H, X = NCH_3, mPip-FTSC (**HL^1**)
R = CH_3, X = NCH_3, mPip-dm-FTSC (**HL^2**)
R = H, X = O, Morph-FTSC (**HL^3**)
R = CH_3, X = O, Morph-dm-FTSC (**HL^4**)

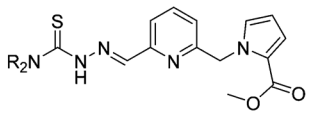

R = H, mPyrr-FTSC (**HL^5**)
R = CH_3, mPyrr-dm-FTSC (**HL^6**)

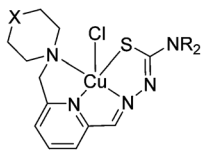

R = H, X = NCH_3, [CuCl(mPipH-FTSC-H)]Cl (**1**+H)Cl[a]
R = CH_3, X = NCH_3, [CuCl(mPipH-dm-FTSC-H)]Cl (**2**+H)Cl
R = H, X = O, [CuCl(Morph-FTSC-H)] (**3**)
R = CH_3, X = O, [CuCl(Morph-dm-FTSC-H)] (**4**)

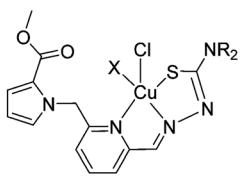

R = H, [CuCl(mPyrr-FTSC-H)(X)] (**5**) X = H_2O (or DMF in X-ray structure)
R = CH_3, [CuCl(mPyrr-dm-FTSC-H)(X)] (**6**) X = H_2O

Chart 1 Hybrid ligands and their copper(II) complexes studied in this work. Underlined numbers indicate complexes studied by X-ray diffraction. Co-crystallized solvent is not included in the formulas (see Experimental section). [a] This complex was crystallized and characterized by X-ray crystallography as [CuCl(mPip-FTSC-H)]·0.15CH_3OH.

terized by analytical and spectroscopic methods (^{1}H and ^{13}C NMR, UV–vis, IR) and X-ray diffraction (**1–5**). Solution equilibria of the copper(II) complexes formed with **HL**[2] and **HL**[4] were studied by pH-potentiometry, UV–vis and EPR spectroscopy and the thermodynamic stability data were compared to those for other related hybrid and non-hybrid systems. The antiproliferative activity of four ligands and four copper(II) complexes has been assayed. The cytotoxicity of **1–4** is markedly lower than that of the parent 2-acetylpyridine and 2-formylpyridine thiosemicarbazones, but significantly higher than that of thiosemicarbazone–proline hybrids and their copper(II) complexes making them pertinent for further development as potential anticancer drugs.

Experimental

Chemicals

2,6-Dihydroxymethylpyridine, 4-methylpiperazine, morpholine and methylpyrrole-2-carboxylate were purchased from Acros Organics. 2-Hydroxymethyl-6-chloromethylpyridine and 6-chloromethylpyridine-2-carboxaldehyde were synthesized according to published protocols.[61] 2-(Chloromethyl)-6-(dimethoxymethyl)pyridine was prepared as described previously.[35] Solvents were dried using standard procedures, if required.[62] KOH, KCl, 4-(2-hydroxyethyl)-1-piperazineethanesulfonic acid (HEPES), 2-(*N*-morpholino)ethanesulfonic acid (MES), ethylenediaminetetraacetic acid (EDTA) were Sigma-Aldrich products, while HCl and $CuCl_2$ were from Reanal. $CuCl_2$ was dissolved in a known amount of HCl in order to get the copper(II) stock solution. Its concentration was determined by complexometric titrations with EDTA.

Synthesis of ligands

1-((6-(Dimethoxymethyl)pyridin-2-yl)methyl)-4-methylpiperazine. 2-(Chloromethyl)-6-(dimethoxymethyl)pyridine (1.82 g, 9.02 mmol) was dissolved in a 1 : 1 mixture of dry THF and dry dichloromethane (40 mL) in a 100 mL Schlenk tube. Methylpiperazine (1.50 mL, 13.53 mmol) and triethylamine (3.64 mL, 27.06 mmol) were added. The reaction mixture was stirred at 46 °C overnight. The next day a white precipitate of triethylammonium chloride was filtered off and washed with THF. The filtrate was concentrated under reduced pressure to yield a brown oily raw product. This was purified on a silica column using chloroform/methanol 4 : 1 as eluent. The solvent was removed under reduced pressure to yield the product as a yellow oil. Yield: 1.99 g, 79%. ^{1}H NMR (500 MHz, DMSO-d_6) δ 7.82 (t, J = 7.7 Hz, 1H, C$H_{(Ar)}$), 7.41 (d, J = 7.7 Hz, 1H, C$H_{(Ar)}$), 7.36 (d, J = 7.7 Hz, 1H, C$H_{(Ar)}$), 5.26 (s, 1H, CH(OCH$_3$)$_2$), 3.60 (s, 2H, CH_2), 3.30 (s, 6H, (OCH_3)$_2$), 2.50–2.35 (m, 8H, C$H_{2(Pip)}$, overlapped with residual DMSO signal), 2.24 (s, 3H, C$H_{3(Pip)}$).

4-((6-(Dimethoxymethyl)pyridin-2-yl)methyl)morpholine. To 2-(Chloromethyl)-6-(dimethoxymethyl)pyridine (0.80 g, 3.97 mmol) in a 1 : 1 mixture of dry THF and dry dichloromethane (20 mL) in a 50 mL Schlenk tube were added morpholine (0.52 mL, 5.96 mmol) and triethylamine (1.60 mL, 11.91 mmol). The reaction mixture was stirred at 46 °C overnight. The next day a white precipitate of triethylammonium chloride was filtered off and washed with THF. The filtrate was concentrated under reduced pressure to yield a brown oily raw product. This was purified on a silica column using chloroform/methanol 97.5 : 2.5 as eluent. The solvent was removed under reduced pressure to yield the product as a yellow oil. Yield: 0.93 g, 93%. ^{1}H NMR (500 MHz, DMSO-d_6) δ 7.82 (t, J = 7.7 Hz, 1H, C$H_{(Ar)}$), 7.44 (d, J = 7.7 Hz, 1H, C$H_{(Ar)}$), 7.36 (d, J = 7.2 Hz, 1H, C$H_{(Ar)}$), 5.26 (s, 1H, CH(OCH$_3$)$_2$), 3.63–3.57 (m, 6H, C$H_{2(Morph)}$, CH_2), 3.30 (s, 6H, (OCH_3)$_2$), 2.44–2.40 (m, 4H, C$H_{2(Morph)}$).

Methyl 1-((6-(dimethoxymethyl)pyridin-2-yl)methyl)-1*H*-pyrrole-2-carboxylate. Sodium hydride (60 wt% dispersion in mineral oil) (0.10 g, 2.48 mmol) was suspended in dry DMF (3 mL) in a 25 mL Schlenk tube and cooled to 0 °C. A solution of methylpyrrole-2-carboxylate (0.31 g, 2.48 mmol) in dry DMF (4.5 mL) was added dropwise. Then a solution of 2-(chloromethyl)-6-(dimethoxymethyl)pyridine (0.50 g, 2.48 mmol) in dry DMF (2.5 mL) was added slowly. The reaction mixture was allowed to reach room temperature and then stirred overnight. The next day the crude mixture was poured into ice water (about 100 mL) and extracted with ethyl acetate (3 × 50 mL). The combined organic phases were dried over magnesium sulfate and the solvent was removed under reduced pressure to give a yellow, oily raw product. This was purified on a silica column using a mixture of 1 : 2 ethyl acetate/hexane as eluent. The product was obtained after removal of the solvent as a colorless oil. Yield: 0.42 g, 58%. ^{1}H NMR (500 MHz, DMSO-d_6) δ 7.76 (t, J = 7.8 Hz, 1H, C$H_{(Ar)}$), 7.35 (d, J = 7.7 Hz, 1H, C$H_{(Ar)}$), 7.31–7.26 (m, 1H, C$H_{(Pyrr)}$), 6.97 (dd, J = 3.9, 1.8 Hz, 1H, C$H_{(Pyrr)}$), 6.60 (d, J = 7.6 Hz, 1H, C$H_{(Ar)}$), 6.24 (dd, J = 3.9, 2.6 Hz, 1H, C$H_{(Pyrr)}$), 5.64 (s, 2H, CH_2), 5.24 (s, 1H, CH(OCH$_3$)$_2$), 3.65 (s, 3H, COOCH_3), 3.31 (s, 6H, (OCH_3)$_2$).

6-((4-Methylpiperazin-1-yl)methyl)picolinaldehyde. A solution of 1-((6-(dimethoxymethyl)pyridin-2-yl)methyl)-4-methylpiperazine (0.93 g, 3.50 mmol) in water (35 mL) and 12 M HCl (0.91 mL, 10.92 mmol) in a 100 mL round-bottom flask was stirred at 60 °C overnight. The next day the reaction mixture was combined with a saturated aqueous solution of sodium bicarbonate (about 100 mL) and extracted with dichloromethane (3 × 40 mL). The united organic phases were dried over magnesium sulfate and the solvent was removed under reduced pressure. The product was obtained as a yellow oil. Yield: 0.51 g, 67%. ^{1}H NMR (500 MHz, DMSO-d_6) δ 9.97 (d, J = 0.7 Hz, 1H, CHO), 8.03 (t, J = 7.7 Hz, 1H, C$H_{(Ar)}$), 7.83 (dd, J = 7.6, 0.9 Hz, 1H, C$H_{(Ar)}$), 7.75 (dd, J = 7.7, 0.9 Hz, 1H, C$H_{(Ar)}$), 3.70 (s, 2H, CH_2), 2.48–2.29 (m, 8H, C$H_{2(Pip)}$), 2.17 (s, 3H, C$H_{3(Pip)}$).

6-(Morpholinomethyl)picolinaldehyde. 4-((6-(Dimethoxymethyl)pyridin-2-yl)methyl) morpholine (0.92 g, 3.65 mmol) was mixed with water (35 mL) and 12 M HCl (0.95 mL, 11.40 mmol) in a 100 mL round-bottom flask. The reaction mixture was stirred at 60 °C overnight. The next day the reaction mixture was combined with a saturated aqueous of sodium bicarbonate (about 100 mL) and extracted with dichloromethane (3 × 40 mL). The united organic phases were dried over magnesium sulfate and the solvent was removed

under reduced pressure. The product was obtained as a yellow oil. Yield: 0.62 g, 82%. ^{1}H NMR (500 MHz, DMSO-d_6) δ 9.98 (d, J = 0.7 Hz, 1H, C*H*O), 8.04 (t, J = 7.7 Hz, 1H, C$H_{(Ar)}$), 7.87–7.81 (m, 1H, C$H_{(Ar)}$), 7.78 (dd, J = 7.7, 1.1 Hz, 1H, C$H_{(Ar)}$), 3.72 (s, 2H, CH_2), 3.64–3.58 (m, 4H, C$H_{2(Morph)}$), 2.47–2.42 (m, 4H, C$H_{2(Morph)}$).

Methyl 1-((6-formylpyridin-2-yl)methyl)-1*H*-pyrrole-2-carboxylate. To a solution of methyl 1-((6-(dimethoxymethyl)pyridin-2-yl)methyl)-1*H*-pyrrole-2-carboxylate (0.21 g, 0.72 mmol) in acetone (5 mL) in a 100 mL round-bottom flask was added water (25 mL) and the reaction mixture was refluxed overnight. The next day the solvent was removed under reduced pressure to yield a white solid, which was further dried *in vacuo*. Yield: 0.18 g, 100%. ^{1}H NMR (500 MHz, DMSO-d_6) δ 9.95 (d, J = 0.7 Hz, 1H, C*H*O), 7.99 (td, J = 7.8, 0.6 Hz, 1H, C$H_{(Ar)}$), 7.82 (dd, J = 7.7, 0.9 Hz, 1H, C$H_{(Ar)}$), 7.36 (dd, J = 2.5, 1.9 Hz, 1H, C$H_{(Pyrr)}$), 7.02–6.92 (m, 2H, C$H_{(Pyrr)}$, C$H_{(Ar)}$), 6.27 (dd, J = 3.9, 2.6 Hz, 1H, C$H_{(Pyrr)}$), 5.76 (s, 2H, CH_2), 3.66 (s, 3H, COOCH_3).

mPip-FTSC·0.2CH$_3$OH (HL^1·0.2CH$_3$OH). A suspension of 6-((4-methylpiperazin-1-yl)methyl) picolinaldehyde (500 mg, 2.28 mmol) and thiosemicarbazide (208 mg, 2.28 mmol) in dry ethanol (6 mL) in a 25 mL Schlenk tube was stirred at 78 °C overnight. The color of the reaction mixture changed from yellow/orange to red/purple. The next day the solvent was removed under reduced pressure and the crude product was purified on preparative HPLC (water/methanol). The product was obtained as a pale-green powder after drying *in vacuo*. Yield: 0.51 g, 76%. Anal. Calcd for $C_{13}H_{20}N_6S·0.2CH_3OH$ (M 298.81 g mol^{-1}): C, 53.05; H, 7.01; N, 28.12; S, 10.73. Found: C, 53.13; H, 6.88; N, 28.28; S, 10.35. *E*-isomer: ^{1}H NMR (500 MHz, DMSO-d_6) δ 11.63 (s, 1H, H^2), 8.33 (s, 1H, H^3), 8.19–8.09 (m, 2H, H^6, H^3), 8.06–8.01 (m, 1H, H^{12}), 7.79 (t, J = 7.8 Hz, 1H, H^5), 7.39 (m, 1H, H^4), 3.57 (s, 2H, H^7), 2.35 (m, 8H, H^8, H^9, H^{10}, H^{11}), 2.15 (s, 3H, H^{14}). ^{13}C NMR (126 MHz, DMSO-d_6) δ 178.80 (Cq, C^{13}), 158.80 (Cq, C^3), 153.13 (Cq, C^1), 143.07 (CH, C^{12}), 137.35 (CH, C^5), 123.44 (CH, C^4), 118.97 (CH, C^6), 64.02 (CH$_2$, C^7), 55.18 (2CH$_2$, C^9, C^{10}), 53.21 (2CH$_2$, C^8, C^{11}), 46.22 (CH$_3$, C^{14}). *Z*-isomer: ^{1}H NMR (500 MHz, DMSO-d_6) δ 14.27 (s, 1H, H^2), 8.51 (s, 1H, H^3), 8.19–8.09 (m, 1H, H^3), 8.06–8.01 (m, 1H, H^5), 7.64 (d, J = 7.5 Hz, 1H, H^6), 7.55 (d, J = 7.6 Hz, 1H, H^4), 7.41–7.35 (m, 1H, H^{12}), 3.70 (s, 2H, H^7), 2.49–2.21 (m, 8H, H^8, H^9, H^{10}, H^{11}), 2.15 (s, 3H, H^{14}). ^{13}C NMR (126 MHz, DMSO-d_6) δ 179.34 (Cq, C^{13}), 157.93 (Cq, C^3), 151.62 (Cq, C^1), 139.16 (CH, C^5), 133.91 (CH, C^{12}), 125.26 (CH, C^6), 124.18 (CH, C^4), 63.79 (CH$_2$, C^7), 55.18 (2CH$_2$, C^9, C^{10}), 53.08 (2CH$_2$, C^8, C^{11}), 46.22 (CH$_3$, C^{14}). For atom numbering and structures of *E* and *Z* isomers see ESI, Scheme S1.† Solubility in water ≥3.3 mg mL^{-1}. Electrospray ionization mass spectrometry (ESI-MS, methanol), positive: m/z 293 ([M + H]$^+$). IR (attenuated total reflectance (ATR), selected bands, $\tilde{\nu}_{max}$): 3420, 3258, 3162, 2940, 2802, 1599, 1546, 1446, 1342, 1280, 1146, 983, 924, 832, 789, 732, 684 cm^{-1}. UV–vis in water (52 μM), λ, nm (ε, M^{-1} cm^{-1}): 315 (30 681).

mPip-dm-FTSC·0.25CH$_3$OH (HL^2·0.25CH$_3$OH). A suspension of 6-((4-methylpiperazin-1-yl)methyl)picolinaldehyde (405 mg, 1.85 mmol) and 4,4-dimethyl-3-thiosemicarbazide (220 mg, 1.85 mmol) in dry ethanol (6 mL) in a 25 mL Schlenk tube was stirred at room temperature overnight. The next day the solvent was removed under reduced pressure and the crude product was purified on preparative HPLC (water/methanol). The product was obtained as a yellow powder after drying *in vacuo*. Yield: 0.52 g, 87%. Anal. Calcd for $C_{15}H_{24}N_6S·0.25CH_3OH$ (M 328.47 g mol^{-1}): C, 55.76; H, 7.67; N, 25.59; S, 9.76. Found: C, 55.93; H, 7.59; N, 25.90; S, 9.38. *E*-isomer: ^{1}H NMR (500 MHz, DMSO-d_6) δ 11.16 (s, 1H, H^2), 8.18 (s, 1H, H^{12}), 7.84–7.71 (m, 2H, H^6, H^5), 7.39 (d, J = 7.3 Hz, 1H, H^4), 3.57 (s, 2H, H^7), 3.31 (s, 6H, H^{14}, H^{15}), 2.47–2.19 (m, 8H, H^8, H^9, H^{10}, H^{11}), 2.15 (s, 3H, H^{16}). ^{13}C NMR (126 MHz, DMSO-d_6) δ 181.10 (Cq, C^{13}), 158.93 (Cq, C^3), 153.36 (Cq, C^1), 144.32 (CH, C^{12}), 137.55 (CH, C^5), 123.22 (CH, C^4), 118.25 (CH, C^6), 64.04 (CH$_2$, C^7), 55.19 (2CH$_2$, C^9, C^{10}), 53.20 (2CH^2, C^8, C^{11}), 46.22 (CH$_3$, C^{16}), 42.83 (2CH$_3$, C^{14}, C^{15}). *Z*-isomer: ^{1}H NMR (500 MHz, DMSO-d_6) δ 14.89 (s, 1H, H^2), 8.05 (t, J = 7.8 Hz, 1H, H^5), 7.65 (d, J = 7.7 Hz, 1H, H^6), 7.59 (s, 1H, H^{12}), 7.53 (d, J = 7.7 Hz, 1H, H^4), 3.62 (s, 2H, H^7), 3.42 (s, 6H, H^{14}, H^{15}), 2.47–2.19 (m, 8H, H^8, H^9, H^{10}, H^{11}), 2.15 (s, 3H, H^{16}). ^{13}C NMR (126 MHz, DMSO-d_6) δ 180.62 (Cq, C^{13}), 157.65 (Cq, C^3), 151.94 (Cq, C^1), 139.25 (CH, C^5), 136.62 (CH, C^{12}), 124.94 (CH, C^6), 124.30 (CH, C^4), 63.66 (CH$_2$, C^7), 55.08 (2CH$_2$, C^9, C^{10}), 53.25 (2CH^2, C^8, C^{11}), 46.18 (CH$_3$, C^{16}), 40.59 (2CH$_3$, C^{14}, C^{15}, overlapped with residual DMSO signal). For atom numbering and structures of *E* and *Z* isomers see ESI, Scheme S1.† Solubility in water ≥11.5 mg mL^{-1}. ESI-MS (methanol), positive: m/z 321 ([M + H]$^+$). IR (ATR, selected bands, $\tilde{\nu}_{max}$): 3039, 2929, 2801, 1597, 1542, 1446, 1361, 1156, 821, 711, 618 cm^{-1}. UV–vis in water (51 μM), λ, nm (ε, M^{-1} cm^{-1}): 216 (20 784), 271sh (14 510), 314 (31 569).

Morph-FTSC·0.3CH$_3$OH·0.1H$_2$O (HL^3·0.3CH$_3$OH·0.1H$_2$O). A suspension of 6-(morpholinomethyl)picolinaldehyde (300 mg, 1.45 mmol) and thiosemicarbazide (132 mg, 1.45 mmol) in dry ethanol (5 mL) in a 25 mL Schlenk tube was stirred at 78 °C overnight. The next day the solvent was removed under reduced pressure and the crude product was recrystallized from water/methanol (5 : 1) to give a white powder which was filtered off, washed with water and dried *in vacuo*. Yield: 0.37 g, 91%. Anal. Calcd for $C_{12}H_{17}N_5O_2S·0.3CH_3OH·0.1H_2O$ (M 306.78 g mol^{-1}): C, 48.16; H, 6.05; N, 22.83; S, 10.45. Found: C, 48.11; H, 6.43; N, 23.13; S, 10.66. *E*-isomer: ^{1}H NMR (500 MHz, DMSO-d_6) δ 11.63 (s, 1H, H2), 8.33 (s, 1H, H3), 8.16 (m, 2H, H6, H3), 8.08–7.99 (m, 1H, H12), 7.80 (t, J = 7.8 Hz, 1H, H5), 7.42 (d, J = 7.6 Hz, 1H4), 3.66–3.52 (m, 6H, H7, H9, H10), 2.42 (m, 4H, H8, H11). ^{13}C NMR (126 MHz, DMSO-d_6) δ 178.81 (Cq, C^{13}), 158.35 (Cq, C^3), 153.20 (Cq, C^1), 143.03 (CH, C^{12}), 137.37 (CH, C^5), 123.58 (CH, C^4), 119.05 (CH, C^6), 66.66 (2CH$_2$, C^9, C^{10}), 64.37 (CH$_2$, C^7), 53.79 (2CH$_2$, C^8, C^{11}). *Z*-isomer: ^{1}H NMR (500 MHz, DMSO-d_6) δ 14.26 (s, 1H, H^2), 8.52 (s, 1H, H^3), 8.16 (m, 1H, H^3), 8.08–7.99 (m, 1H, H^5), 7.65 (d, J = 7.5 Hz, 1H, H^6), 7.58 (d, J = 7.8 Hz, 1H, H^4), 7.39 (s, 1H, H^{12}), 3.71 (s, 2H, H^7), 3.66–3.52 (m, 4H, H^9, H^{10}), 2.48 (m, 4H, H^8, H^{11}). ^{13}C NMR (126 MHz, DMSO-d_6) δ 179.37 (Cq, C^{13}), 157.51 (Cq, C^3), 151.68 (Cq, C^1), 139.19 (CH, C^5), 133.91 (CH, C^{12}), 125.31 (CH, C^6), 124.30 (CH, C^4), 66.66 (2CH$_2$, C^9, C^{10}),

64.10 (CH_2, C^7), 53.69 ($2CH_2$, C^8, C^{11}). For atom numbering and structures of *E* and *Z* isomers see ESI, Scheme S1.† Solubility in water (with 1% DMSO) ≥1.4 mg mL^{-1}. ESI-MS (methanol), positive: *m*/*z* 280 ($[M + H]^+$). IR (ATR, selected bands, $\tilde{\nu}_{max}$): 3462, 3268, 3167, 2816, 1611, 1522, 1452, 1261, 1109, 1067, 850, 645 cm^{-1}. UV–vis in water (39 μM), λ, nm (ε, M^{-1} cm^{-1}): 316 (26 923).

Morph-dm-FTSC (HL^4). A suspension of 6-(morpholinomethyl)picolinaldehyde (300 mg, 1.45 mmol) and 4,4-dimethyl-3-thiosemicarbazide (173 mg, 1.45 mmol) in dry ethanol (5 mL) in a 25 mL Schlenk tube was stirred at room temperature overnight. The next day a white precipitate was filtered off under inert conditions. The precipitate was washed with dry ethanol (1 mL) and dried *in vacuo* to give a white powder. Yield: 0.34 g, 76%. Anal. Calcd for $C_{14}H_{21}N_5OS$ (M 307.42 g mol^{-1}): C, 54.70; H, 6.89; N, 22.78; S, 10.43. Found: C, 54.85; H, 6.92; N, 22.71; S, 10.28. *E*-isomer: ^{1}H NMR (500 MHz, DMSO-d_6) δ 11.16 (s, 1H, H^2), 8.18 (s, 1H, H^{12}), 7.84–7.74 (m, 2H, H^5, H^6), 7.44–7.39 (m, 1H, H^4), 3.62–3.53 (m, 6H, H^7, H^9, H^{10}), 3.31 (s, 6H, H^{14}, H^{15}), 2.45–2.40 (m, 4H, H^8, H^{11}). ^{13}C NMR (126 MHz, DMSO-d_6) δ 181.07 (Cq, C13), 158.49 (Cq, C^3), 153.45 (Cq, C_1), 144.30 (CH, C^{12}), 137.58 (CH, C^5), 123.34 (CH, C^4), 118.32 (CH, C^6), 66.67 ($2CH_2$, C^9, C^{10}), 64.38 (CH_2, C^7), 53.78 ($2CH_2$, C^8, C^{11}), 42.84 ($2CH_3$, C^{14}, C^{15}). *Z*-isomer: ^{1}H NMR (500 MHz, DMSO-d_6) δ 14.88 (s, 1H, H^2), 8.05 (t, *J* = 7.8 Hz, 1H, H^5), 7.66 (d, *J* = 7.7 Hz, 1H, H^6), 7.59 (s, 1H, H^{12}), 7.56 (d, *J* = 7.7 Hz, 1H. H^4), 3.63 (s, 2H, H^7), 3.62–3.53 (m, 4H, H^9, H^{10}), 3.42 (s, 6H, H^{14}, H^{15}), 2.40–2.35 (m, 4H, H^{11}, H^8). ^{13}C NMR (126 MHz, DMSO-d_6) δ 180.61 (Cq, C^{13}), 157.21 (Cq, C^3), 152.00 (Cq, C^1), 139.27 (CH, C^5), 136.59 (CH, C^{12}), 125.02 (CH, C^6), 124.41 (CH, C^4), 66.58 ($2CH_2$, C^9, C^{10}), 64.01 (CH_2, C^7), 53.78 ($2CH_2$, C^8, C^{11}), 40.63 ($2CH_3$, C^{14}, C^{15}, overlapped with residual DMSO signal). For atom numbering and structures of *E* and *Z* isomers see ESI, Scheme S1.† Solubility in water ≥2.6 mg mL^{-1}. ESI-MS (methanol), positive: *m*/*z* 308 ($[M + H]^+$). IR (ATR, selected bands, $\tilde{\nu}_{max}$): 2923, 2821, 1593, 1532, 1313, 1145, 1107, 901, 821, 707, 622 cm^{-1}. UV–vis in water (48 μM), λ, nm (ε, M^{-1} cm^{-1}): 216 (19 628), 273 (13 430), 315 (21 488).

mPyrr-FTSC (HL^5). A suspension of methyl 1-((6-formylpyridin-2-yl)methyl)-1*H*-pyrrole-2-carboxylate (0.06 g, 0.24 mmol) and thiosemicarbazide (0.02 g, 0.24 mmol) in a 1 : 1 mixture of methanol/ethanol (2 mL) in a 10 mL Schlenk tube was stirred at 78 °C overnight. The next day the solvent was removed under reduced pressure and the crude product was recrystallized from water/methanol (5 : 1). The resulting white powder was filtered off, washed with a water/methanol 1 : 1 mixture and dried *in vacuo*. Yield: 0.06 g, 76%. Anal. Calcd for $C_{14}H_{15}N_5O_2S$ (M 317.37 g mol^{-1}): C, 52.98; H, 4.76; N, 22.07; S, 10.10. Found: C, 52.98; H, 4.65; N, 21.97; S, 10.00. *E*-isomer: ^{1}H NMR (500 MHz, DMSO-d_6) δ 11.66 (s, 1H, H^2), 8.35 (s, 1H, H^3), 8.20–8.11 (m, 2H, H^3, H^6), 8.04 (s, 1H, H^{13}), 7.75 (t, *J* = 7.9 Hz, 1H, H^{13}), 7.33–7.29 (m, 1H, H^9), 7.00–6.92 (m, 1H, H^{11}), 6.60 (d, *J* = 7.7 Hz, 1H, H^4), 6.28–6.21 (m, 1H, H^{10}), 5.64 (s, 2H, H^7), 3.66 (s, 3H, H^{15}). ^{13}C NMR (126 MHz, DMSO-d_6) δ 178.84 (Cq, C^{15}), 161.08 (Cq, C^{12}), 158.54 (Cq, C^3), 153.30 (Cq, C^1), 142.66 (CH, C^{13}), 137.99 (CH, C^5), 131.10 (CH, C^9), 121.65 (Cq, C^8), 120.41 (CH, C^4), 119.08 (CH, C^6), 118.61 (CH, C^{11}), 109.05 (CH, C^{10}), 53.37 (CH_2, C^7), 51.39 (CH_3, C^{15}). *Z*-isomer: ^{1}H NMR (500 MHz, DMSO-d_6) δ 14.05 (s, 1H, H^2), 8.60 (s, 1H, H^3), 8.24 (s, 1H, H^3), 8.00 (t, *J* = 7.8 Hz, 1H, H^5), 7.66 (d, *J* = 7.6 Hz, 1H, H^6), 7.64–7.59 (m, 1H, H^9), 7.40 (s, 1H, H^{13}), 6.98–6.91 (m, 2H, H^4, H^{11}), 6.28–6.21 (m, 1H, H^{10}), 5.69 (s, 2H, H^7), 3.68 (s, 3H, H^{15}). ^{13}C NMR (126 MHz, DMSO-d_6) δ 179.40 (Cq, C^{14}), 161.08 (Cq, C^{12}), 157.34 (Cq, C^3), 151.83 (Cq, C^1), 139.84 (CH, C^5), 133.66 (CH, C^{13}), 131.63 (CH, C^9), 125.65 (CH, C^6), 122.07 (CH, C^4), 121.30 (Cq, C^8), 118.95 (CH, C^{11}), 109.37 (CH, C^{10}), 53.37 (CH_2, C^7), 51.47 (CH_3, C^{15}). ESI-MS (methanol), positive: *m*/*z* 340 ($[M + Na]^+$), 317 ($[M + H]^+$). IR (ATR, selected bands, $\tilde{\nu}_{max}$): 3561, 3353, 3243, 2972, 1706, 1612, 1530, 1443, 1245, 723, 653, 608 cm^{-1}. UV–vis in methanol (22 μM), λ, nm (ε, M^{-1} cm^{-1}): 204 (13 636), 237 (12 182), 266 (17 227), 324 (25 545), 388 (1227).

mPyrr-dm-FTSC (HL^6). A solution of methyl 1-((6-formylpyridin-2-yl)methyl)-1*H*-pyrrole-2-carboxylate (0.18 g, 0.72 mmol) and 4,4-dimethyl-3-thiosemicarbazide (0.09 g, 0.72 mmol) in a 1 : 1 mixture of methanol/ethanol (4 mL) in a 25 mL Schlenk tube was stirred at room temperature for 6 h. The white precipitate was filtered off, washed with a water/methanol 1 : 1 mixture and dried *in vacuo*. Yield: 0.12 g, 47%. Anal. Calcd for $C_{16}H_{19}N_5O_2S$ (M 345.42 g mol^{-1}): C, 55.63; H, 5.54; N, 20.27; S, 9.28. Found: C, 55.43; H, 5.50; N, 20.06; S, 9.21. *E*-isomer: ^{1}H NMR (500 MHz, DMSO-d_6) δ 11.18 (s, 1H, H^2), 8.17 (s, 1H, H^{13}), 7.79–7.73 (m, 2H, H^6, H^5), 7.33–7.27 (m, 1H, H^9), 6.96 (dd, *J* = 3.9, 1.8 Hz, 1H, H^{11}), 6.69–6.62 (m, 1H, H^4), 6.23 (dd, *J* = 3.9, 2.6 Hz, 1H, H^{10}), 5.65 (s, 2H, H^7), 3.66 (s, 3H, H^{17}), 3.31 (s, 6H, H^{15}, H^{16}). ^{13}C NMR (126 MHz, DMSO-d_6) δ 180.99 (Cq, C^{14}), 161.06 (Cq, C^{12}), 158.57 (Cq, C^3), 153.55 (Cq, C^1), 144.09 (CH, C^{13}), 138.14 (CH, C^5), 131.12 (CH, C^9), 121.66 (Cq, C^8), 120.34 (CH, C^4), 118.56 (CH, C^{11}), 118.35 (CH, C^6), 108.96 (CH, C^{10}), 53.40 (CH_2, C^7), 51.38 (CH_3, C^{17}), 42.76 ($2CH_3$, C^{15}, C^{16}). *Z*-isomer: ^{1}H NMR (500 MHz, DMSO-d_6) δ 14.71 (s, 1H, H^2), 7.99 (t, *J* = 7.9 Hz, 1H, H^5), 7.65 (d, *J* = 7.7 Hz, 1H, H^6), 7.62 (s, 1H, H^{13}), 7.40–7.35 (m, 1H, H^9), 7.02 (dd, *J* = 4.0, 1.8 Hz, 1H, H^{11}), 6.49 (d, *J* = 7.8 Hz, 1H, H^4), 6.30 (dd, *J* = 3.9, 2.6 Hz, 1H, H^{10}), 5.73 (s, 2H, H^7), 3.64 (s, 3H, H^{17}), 3.44 (s, 6H, H^{15}, H^{16}). ^{13}C NMR (126 MHz, DMSO-d_6) δ 180.60 (Cq, C^{14}), 161.01 (Cq, C^{12}), 158.01 (Cq, C^3), 151.49 (Cq, C^1), 140.11 (CH, C^5), 136.28 (CH, C^{13}), 131.12 (CH, C^9), 124.83 (CH, C^6), 121.66 (Cq, C^8), 120.10 (CH, C^4), 118.94 (CH, C^{11}), 109.49 (CH, C^{10}), 53.40 (CH_2, C^7), 51.51 (CH_3, C^{17}), 40.60 (C^{15}, C^{16}, overlapped with residual DMSO signal). For atom numbering and structures of *E* and *Z* isomers see ESI, Scheme S1.† ESI-MS (methanol), positive: *m*/*z* 368 ($[M + Na]^+$), 346 ($[M + H]^+$). IR (ATR, selected bands, $\tilde{\nu}_{max}$): 2837, 1693, 1541, 1316, 1252, 1106, 899, 757, 622 cm^{-1}. UV–vis in methanol (28 μM), λ, nm (ε, M^{-1} cm^{-1}): 235 (23 929), 266 (27 321), 321 (21 786), 405 (2757).

Synthesis of the copper(II) complexes

[CuCl(mPipH-FTSC-H)]Cl·0.1H_2O ((1 + H)Cl·0.1H_2O). To a solution of mPip-FTSC (**HL^1**) (0.05 g, 0.17 mmol) in methanol

(20 mL) was added a solution of copper(II) chloride dihydrate (0.03 g, 0.17 mmol) in methanol (5 mL). The reaction mixture was stirred at room temperature overnight. The next day a green precipitate was filtered off, washed with methanol and dried *in vacuo*. Yield: 0.05 g, 74%. Anal. Calcd for $C_{13}H_{20}Cl_2CuN_6S{\cdot}0.1H_2O$ (M 428.66 g mol^{-1}): C, 36.43; H, 4.75; N, 19.61; S, 7.48. Found: C, 36.49; H, 4.74; N, 19.24; S, 7.48. Solubility in water ≥13.2 mg mL^{-1}. ESI-MS (methanol), positive: *m*/*z* 354 ([M − Cl]$^+$). IR (ATR, selected bands, $\tilde{\nu}_{max}$): 3266, 3094, 1613, 1459, 1418, 1158, 1025, 978, 825, 787, 653 cm^{-1}. UV–vis in water, λ, nm (ε, M^{-1} cm^{-1}): 286 (19 545), 392 (10 063) (measured at 44 μM); 607 (265) (measured at 1.88 mM). X-ray diffraction quality crystals of the composition **1**·0.15CH_3OH were obtained after slow diffusion of diethyl ether into a methanolic solution of **1** ($c \approx 5$ mg mL^{-1}) in the presence of a small amount of triethylamine.

[CuCl(mPipH-dm-FTSC-H)]Cl·0.9H_2O·0.5CH_3OH ((2 + H)Cl·0.9H_2O·0.5CH_3OH). To a solution of mPip-dm-FTSC (**HL^2**) (0.17 g, 0.53 mmol) in methanol (20 mL) was added a solution of copper(II) chloride dihydrate (0.10 g, 0.58 mmol) in methanol (5 mL) and triethylamine (80.8 μL, 0.64 mmol). The reaction mixture was stirred at room temperature overnight. The next day the solvent was concentrated under reduced pressure to about 10 mL. After slow diffusion of diethyl ether green crystals appeared which were filtered off, washed with methanol and dried *in vacuo*. The obtained crystals were of X-ray diffraction quality. Yield: 0.14 g, 53%. Anal. Calcd for $C_{15}H_{24}Cl_2CuN_6S{\cdot}0.9H_2O{\cdot}0.5CH_3OH$ (M 487.14 g mol^{-1}): C, 38.22; H, 5.75; N, 17.25; S, 6.58. Found: C, 38.23; H, 5.40; N, 17.37; S, 6.43. Solubility in water ≥20.2 mg mL^{-1}. ESI-MS (methanol), positive: *m*/*z* 382 ([M − Cl]$^+$). IR (ATR, selected bands, $\tilde{\nu}_{max}$): 3458, 3394, 3037, 2690, 1492, 1369, 1311, 1249, 1130, 908, 612 cm^{-1}. UV–vis in water, λ, nm (ε, M^{-1} cm^{-1}): 254 (11 463), 299 (17 561), 405 (15 366) (measured at 41 μM); 574 (145) (measured at 1.79 mM).

[CuCl(Morph-FTSC-H)]·2H_2O·0.2C_2H_5OH (3·2H_2O·0.2C_2H_5OH). To a solution of Morph-FTSC (**HL^3**) (0.15 g, 0.54 mmol) in ethanol (35 mL) were added a solution of copper(II) chloride dihydrate (0.09 g, 0.54 mmol) in ethanol (5 mL) and triethylamine (75 μL, 0.54 mmol). The reaction mixture was stirred at room temperature overnight. The next day a green precipitate was filtered off, washed with ethanol and dried *in vacuo*. X-ray diffraction quality crystals were obtained after slow diffusion of diethyl ether into a methanolic solution of **3** ($c \approx 5$ mg mL^{-1}). Yield: 0.20 g, 88%. Anal. Calcd for $C_{12}H_{16}ClCuN_5OS{\cdot}2H_2O{\cdot}0.2C_2H_5OH$ (M 422.60 g mol^{-1}): C, 35.24; H, 5.06; N, 16.57; S, 7.59. Found: C, 35.35; H, 4.81; N, 16.42; S, 7.61. Solubility in water ≥1.1 mg mL^{-1}. ESI-MS (methanol), positive: *m*/*z* 341 ([M − Cl]$^+$). IR (ATR, selected bands, $\tilde{\nu}_{max}$): 3431, 3367, 3109, 1677, 1640, 1462, 1419, 1166, 1114, 783, 630 cm^{-1}. UV–vis in water, λ, nm (ε, M^{-1} cm^{-1}): 284 (20 179), 389 (10 893) (measured at 56 μM); 598 (252) (measured at 2.83 mM).

[CuCl(Morph-dm-FTSC-H)]·0.2H_2O·0.6CH_3OH (4·0.2H_2O·0.6CH_3OH). To a solution of Morph-dm-FTSC (**HL^4**) (0.15 g, 0.49 mmol) in methanol (20 mL) were added a solution of copper(II) chloride dihydrate (0.08 g, 0.49 mmol) in methanol (5 mL) and triethylamine (68 μL, 0.49 mmol). The reaction mixture was stirred at room temperature overnight. The next day the solvent was removed under reduced pressure to about 10 mL. After slow diffusion of diethyl ether green crystals appeared which were filtered off, washed with methanol and dried *in vacuo*. The obtained crystals were of X-ray diffraction quality. Yield: 0.21 g, 98%. Anal. Calcd for $C_{14}H_{20}ClCuN_5OS{\cdot}0.2H_2O{\cdot}0.6CH_3OH$ (M 428.23 g mol^{-1}): C, 40.95; H, 5.37; N, 16.35; S, 7.49. Found: C, 40.84; H, 5.29; N, 16.23; S, 7.57. Solubility in water ≥12.9 mg mL^{-1}. ESI-MS (methanol), positive: *m*/*z* 369 ([M − Cl]$^+$). IR (ATR, selected bands, $\tilde{\nu}_{max}$): 3499, 2859, 1593, 1359, 1242, 1123, 909, 869, 789 cm^{-1}. UV–vis in water, λ, nm (ε, M^{-1} cm^{-1}): 255 (10 474), 299 (17 207), 405 (15 212) (measured at 40 μM); 575 (293) (measured at 1.78 mM).

[CuCl(mPyrr-FTSC-H)(H_2O)]·0.2H_2O (5·0.2H_2O). To a solution of mPyrr-FTSC (**HL^5**) (0.05 g, 0.16 mmol) in methanol (15 mL) was added a solution of copper(II) chloride dihydrate (0.03 g, 0.17 mmol) in methanol (7 mL). The reaction mixture was stirred at 60 °C for 1 h and then allowed to stand at 4 °C for 2 h. A green microcrystalline precipitate was filtered off, washed with methanol and dried *in vacuo*. X-ray diffraction quality crystals were obtained after slow diffusion of diethyl ether into a DMF solution of **5** ($c \approx 5$ mg mL^{-1}). Yield: 0.05 g, 71%. Anal. Calcd for $C_{14}H_{16}ClCuN_5O_3S{\cdot}0.2H_2O$ (M 436.98 g mol^{-1}): C, 38.48; H, 3.78; N, 16.03; S, 7.34. Found: C, 38.76; H, 3.39; N, 15.75; S, 7.05. ESI-MS (methanol), positive: *m*/*z* 379 ([M − Cl − H_2O]$^+$). IR (ATR, selected bands, $\tilde{\nu}_{max}$): 3346, 3105, 1704, 1622, 1463, 1406, 1332, 1253, 1111, 734, 635 cm^{-1}. UV–vis in DMF, λ, nm (ε, M^{-1} cm^{-1}): 298 (16 447), 326 (13 026, sh), 422 (11 474) (measured at 76 μM); 514 (274, sh), 684 (225) (measured at 2.29 mM).

[CuCl(mPyrr-dm-FTSC-H)(H_2O)] (6). To a warm solution of mPyrr-dm-FTSC (**HL^6**) (0.07 g, 0.20 mmol) in methanol a solution of copper(II) chloride dihydrate (0.04 g, 0.20 mmol) was added. The formation of a green precipitate started immediately and the reaction mixture was allowed to stir at room temperature overnight. The next day the green precipitate was filtered off, washed extensively with methanol and dried *in vacuo*. Yield: 0.05 g, 55%. Anal. Calcd for $C_{16}H_{20}ClCuN_5O_3S$ (M 461.43 g mol^{-1}): C, 41.65; H, 4.37; N, 15.18; S, 6.94. Found: C, 41.80; H, 4.35; N, 15.04; S, 6.81. ESI-MS (methanol), positive: *m*/*z* 407 ([M − Cl − H_2O]$^+$). IR (ATR, selected bands, $\tilde{\nu}_{max}$): 3420, 3006, 1705, 1508, 1377, 1246, 1113, 913, 735, 587 cm^{-1}. UV–vis in DMF, λ, nm (ε, M^{-1} cm^{-1}): 306 (13 851), 426 (15 946) (measured at 74 μM); 519 (435), 648 (256) (measured at 2.21 mM).

pH-Potentiometric measurements

The purity and aqueous phase stability of the ligands mPip-dm-FTSC (**HL^2**) and Morph-dm-FTSC (**HL^4**) were verified and the exact concentrations of the stock solutions prepared were determined by the Gran method.[63] The pH-metric measurements for determination of the protonation constants of the ligands and the overall stability constants of the copper(II) complexes were carried out at 298.0 ± 0.1 K in water and at an

ionic strength of 0.10 M (KCl) in order to keep the activity coefficients constant. The titrations were performed with carbonate-free KOH solution of known concentration (0.10 M). The concentrations of the KOH and the HCl were determined by pH-potentiometric titrations. An Orion 710A pH-meter equipped with a Metrohm combined electrode (type 6.0234.100) and a Metrohm 665 Dosimat burette were used for the pH-metric measurements. The electrode system was calibrated to the pH = $-\log[H^+]$ scale in water according to the method suggested by Irving *et al.*[64] The average water ionization constant pK_w, is 13.76 ± 0.01, which corresponds well to the literature data.[65] The reproducibility of the titration points included in the calculations was within 0.005 pH. The pH-metric titrations were performed in the pH range 2.0–11.5. The initial volume of the samples was 5.0 mL. The concentration of the ligands was 2 mM and metal ion-to-ligand ratios of 1 : 1, 1 : 1.5, 1 : 2 and 1 : 3 were used. The accepted fitting of the titration curves was always less than 0.01 mL. Samples were deoxygenated by bubbling purified argon through them for *ca.* 10 min prior to the measurements and argon was also passed over the solutions during the titrations.

The protonation constants of the ligands were determined with the computer program HYPERQUAD.[66] PSEQUAD[67] was utilized to establish the stoichiometry of the complexes and to calculate the stability constants ($\log\beta(M_pL_qH_r)$). $\beta(M_pL_qH_r)$ is defined for the general equilibrium $pM + qL + rH \rightleftharpoons M_pL_qH_r$ as $\beta(M_pL_qH_r) = [M_pL_qH_r]/[M]^p[L]^q[H]^r$, where M denotes the metal ion (copper(II)) and L the completely deprotonated ligand. In all calculations exclusively titration data were used from experiments, in which no precipitate was visible in the reaction mixture.

UV–vis spectrophotometric, spectrofluorimetric and ^{1}H NMR measurements

A Thermo Scientific Evolution 220 spectrophotometer was used to record the UV–vis spectra in the 200 to 1050 nm window. The path length was 1 or 0.5 cm. Stability constants and the individual spectra of the complexes were calculated by the computer program PSEQUAD.[67] The spectrophotometric titrations were performed on samples of the copper(II) complexes **2** and **4** of ligands mPip-dm-FTSC (**HL^2**) and Morph-dm-FTSC (**HL^4**) over the pH range between 2 and 11.5 at an ionic strength of 0.10 M (KCl) in water at 298.0 ± 0.1 K. The concentration of the metal complexes was 2.5 mM. Measurements on the copper(II) complexes **2** and **4** were also carried out by preparing individual samples, in which the 0.1 M KCl was partially or completely replaced by HCl and pH values, varying in the range of approximately 1.0–3.0, were calculated from the HCl content. The conditional stability constants of [CuL] at pH 7.4 (10 mM HEPES) for **2** and at pH 5.6 (10 mM MES) for **4** were determined from competition titrations of the copper(II) complex of EDTA with the ligands **HL^2** and **HL^4**. Samples contained 50 μM copper(II) ion and 50 μM EDTA, and the concentration of the ligands **HL^2** and **HL^4** was varied in the range of 0–170 μM. Absorbance data recorded after 1.5 h incubation time in the wavelength interval from 415 to 450 nm were used for the calculations.

Three-dimensional fluorescence spectra of the ligands mPip-dm-FTSC (**HL^2**) and Morph-dm-FTSC (**HL^4**) and their copper(II) complexes (**2** and **4**) were recorded at 240–500 nm excitation and at 300–700 nm emission wavelengths for the 10 μM ligand containing samples in 1 cm quartz cell at pH 7.4 (10 mM HEPES) using 5 nm/5 nm slit widths at 0.1 M (KCl) ionic strength and 298.0 ± 0.1 K.

The pH-dependent ^{1}H NMR studies were carried out on a Bruker Ultrashield 500 Plus instrument. 4,4-Dimethyl-4-silapentane-1-sulfonic acid was used as an internal NMR standard. Ligands mPip-dm-FTSC (**HL^2**) and Morph-dm-FTSC (**HL^4**) were dissolved in a 10% (v/v) D_2O/H_2O mixture in a concentration of 3.0 and 1.5 mM, respectively. The direct pH-meter readings were corrected according to the method of Irving *et al.*[64] Spectra of the ligands were recorded using individual samples, in which the 0.1 M KCl was partially or completely replaced by HCl and pH values, varying in the range of approximately 1.0–2.0, were calculated from the HCl content.

Determination of the distribution coefficients (D)

$D_{7.4}$ values of ligands **HL^1**–**HL^5** and their copper(II) complexes (**1**–**5**) were determined by the traditional shake-flask method in *n*-octanol/buffered aqueous solution at pH 7.4 at 298.0 ± 0.2 K as described previously.[68,69] Two parallel experiments were performed for each sample. The ligands and the complexes were dissolved at 100 μM (~30 μM in the case of **HL^5** and its complex **5**) in the *n*-octanol pre-saturated aqueous solution of the buffer (10 mM HEPES) at constant ionic strength (0.10 M KCl). The aqueous solutions and *n*-octanol with 1 : 1 phase ratio were gently mixed with 360° vertical rotation for 3 h to avoid the emulsion formation, and the mixtures were centrifuged at 5000 rpm for 5 min by a temperature controlled centrifuge (Sanyo) at 298 K. After separation UV–vis spectra of the ligands or complexes in the aqueous phase were compared to those of the original aqueous solutions. Since measurable amounts of the ligand **HL^5** and its copper(II) complex **5** were not found in the aqueous phase after partitioning, their $\log D_{7.4}$ values were merely estimated.

EPR measurements and deconvolution of the spectra

All continuous wave (CW)-EPR spectra were recorded with a BRUKER EleXsys E500 spectrometer (microwave frequency 9.85 GHz, microwave power 10 mW, modulation amplitude 5 G, modulation frequency 100 kHz). The pH-dependent series of isotropic EPR spectra were recorded in a circulating system, at room temperature. A Heidolph Pumpdrive 5101 peristaltic pump was used to transport the solution from the titration pot through a capillary tube into a Bruker flat cell placed in the cavity of the instrument. The EPR titrations were performed over the pH range between 1.5 and 12.0 at an ionic strength of 0.10 M (KCl) under nitrogen atmosphere. Samples contained 1 mM mPip-dm-FTSC (**HL^2**) or Morph-dm-FTSC (**HL^4**) and 1 mM or 0.5 mM copper(II) ions. A 0.1 M KOH solution was added to the samples to adjust the pH, which was measured

with an Orion 710A pH-meter equipped with a Metrohm 6.0234.100 glass electrode. For selected pH values (where predominantly complexes formed) 0.1 mL samples were introduced into quartz EPR tubes and measured individually at 77 K.

Before the simulation, the measured spectra were corrected by subtracting the spectra of water measured in the same circulating system. A phase correction of −7 degree for the series of Morph-dm-FTSC ($\mathbf{HL}^4$) and −8 degree for the mPip-dm-FTSC ($\mathbf{HL}^2$) containing samples was used to correct the phase of the spectra which were probably shifted due to the not perfectly perpendicular position of the flat cell to the magnetic field. Both series of the pH-dependent isotropic CW-EPR spectra were simulated by the "two-dimensional" method using the 2D_EPR program.[70] The parameters g_o, A_o^{Cu} copper hyperfine (I_{Cu} = 3/2) and A_o^N nitrogen (I_N = 1) superhyperfine couplings have been taking into account to describe each component curve. The relaxation parameters, α, β, and γ defined the linewidths through the equation $\sigma_{M_I} = \alpha + \beta M_I + \gamma M_I^2$, where M_I denotes the magnetic quantum number of the paramagnetic metal ions. The equilibrium concentrations of the copper(II) complexes were varied by fitting their overall stability constants $\beta(M_pL_qH_r)$ defined in the section of pH-potentiometric measurements. For each spectrum, the noise-corrected regression parameter (R_j for the j^{th} spectrum) is derived from the average square deviation (SQD) between the experimental and the calculated intensities. For the series of spectra, the fit is characterized by the overall regression coefficient R, calculated from the overall average SQD. The overall regression coefficient was 0.9933 for the series of Morph-dm-FTSC and 0.9928 for the series of mPip-dm-FTSC. The details of the statistical analysis were published previously.[70] The anisotropic EPR spectra, recorded at 77 K, were analyzed individually with the aid of the EPR program.[71] In case of copper(II) complexes, the anisotropic EPR parameters: rhombic g-tensor (g_x, g_y, g_z), rhombic copper(II) hyperfine tensor (A_x^{Cu}, A_y^{Cu}, A_z^{Cu}) and rhombic nitrogen hyperfine tensor (a_x^N, a_y^N, a_z^N, for which x, y and z denotes the directions of the g-tensor) were fitted. For the description of the linewidth the orientation dependent α, β and γ parameters were used to set up each component spectra. Since a natural $CuCl_2$ salt was used for the measurements, both the isotropic and anisotropic spectra were calculated as the sum of the spectra of ^{63}Cu and ^{65}Cu weighted by their natural abundances. The hyperfine and superhyperfine coupling constants and the relaxation parameters were obtained in field units (Gauss = 10^{-4} T).

Crystallographic structure determination

X-ray diffraction measurements were performed on Bruker X8 APEXII CCD and Bruker D8 VENTURE diffractometers. Single crystals were positioned at 35, 35, 40, 35 and 40 mm from the detector, and 1645, 1386, 890, 3033 and 2542 frames were measured, each for 48, 8, 48, 65 and 24 s over 0.4, 0.4, 0.4, 0.5 and 0.4° scan width for **1**·0.15CH_3OH, **2**·2H_2O, **3**·0.5$(C_2H_5)_2O$, **4**·0.93CH_3OH and **5**, respectively. The data were processed using SAINT software.[72] Crystal data, data collection parameters, and structure refinement details are given in Table 1. The structures were solved by direct methods and refined by full-matrix least-squares techniques. Non-H atoms were refined with anisotropic displacement parameters. H atoms were inserted in calculated positions and refined with a riding model. In the crystal structure of **1**·0.15CH_3OH a partly occupied (15%) co-crystallized methanol molecule position was found, while in the crystal structure of **3**·0.5$(C_2H_5)_2O$ half

Table 1 Crystal data and details of data collection for **1**·0.15CH_3OH, **2**·2H_2O, **3**·0.5$(C_2H_5)_2O$, **4**·0.93CH_3OH and **5**

	1·0.15CH_3OH	**2**·2H_2O	**3**·0.5$(C_2H_5)_2O$	**4**·0.93CH_3OH	**5**
Empirical formula	$C_{13.15}H_{19.6}ClCuN_6O_{0.15}S$	$C_{15}H_{28}Cl_2CuN_6O_2S$	$C_{14}H_{21}ClCuN_5O_{1.5}S$	$C_{14.93}H_{23.7}ClCuN_5O_{1.92}S$	$C_{17}H_{21}ClCuN_6O_3S$
Fw	395.20	490.93	414.42	435.04	488.45
Space group	$P2_1/n$	$P\bar{1}$	$P2_1/n$	$P\bar{1}$	$P\bar{1}$
a [Å]	7.6944(5)	7.6629(3)	7.7969(6)	9.8676(7)	8.0848(4)
b [Å]	17.4966(10)	11.7864(3)	17.4139(14)	12.0982(8)	12.1277(6)
c [Å]	13.1409(8)	13.0949(4)	13.145(1)	16.606(1)	12.3563(5)
α [°]		72.114(1)		86.450(3)	63.8664(17)
β [°]	102.615(2)	73.613(1)	103.700(2)	74.015(3)	83.4075(18)
γ [°]		74.311(1)		77.176(3)	73.0771(17)
V [Å^3]	1726.40(18)	1057.72(6)	1734.0(2)	1858.2(2)	1040.45(8)
Z	4	2	4	4	2
λ [Å]	0.71073	0.71073	0.71073	0.71073	0.71073
ρ_{calcd} [g cm^{-3}]	1.520	1.541	1.587	1.555	1.559
Crystal size, mm	0.26 × 0.02 × 0.02	0.17 × 0.10 × 0.04	0.09 × 0.04 × 0.03	0.50 × 0.40 × 0.40	0.10 × 0.08 × 0.06
T [K]	100(2)	100(2)	100(2)	100(2)	100(2)
μ [mm^{-1}]	1.547	1.407	1.548	1.450	1.310
R_1 [a]	0.0334	0.0303	0.0424	0.0279	0.0326
wR_2 [b]	0.0753	0.0832	0.0950	0.0683	0.0745
GOF[c]	1.079	1.033	1.011	1.095	1.040

[a] $R_1 = \sum||F_o| - |F_c||/\sum|F_o|$. [b] $wR_2 = \{\sum[w(F_o^2 - F_c^2)^2]/\sum[w(F_o^2)^2]\}^{1/2}$. [c] GOF = $\{\sum[w(F_o^2 - F_c^2)^2]/(n-p)\}^{1/2}$, where n is the number of reflections and p is the total number of parameters refined.

molecule of diethyl ether per asymmetric unit was found to be disordered over two positions with site occupation factor (s.o.f.) 0.5 : 0.5. In the crystal of **4**·0.93CH_3OH one molecule of co-crystallized methanol is disordered over 3 positions with s.o.f. 0.4 : 0.35 : 0.25, while the second molecule position is populated to 85%. The disorder was solved by using SADI instructions implemented in SHELXL-97, while the atoms involved were refined with isotropic displacement parameters and the positions of H atoms were calculated. The following computer programs were used: structure solution, SHELXS-97 and refinement, SHELXL-97;[73] molecular diagrams, ORTEP.[74] CCDC 1052906–1052910.

Cell lines and culture conditions

Human cervical carcinoma (HeLa), human alveolar basal adenocarcinoma (A549), human colon carcinoma (LS174) cell lines and normal human foetal lung fibroblast cell line (MRC-5) were maintained as a monolayer culture in the Roswell Park Memorial Institute (RPMI) 1640 nutrient medium (Sigma Chemicals Co, USA). RPMI 1640 nutrient medium was prepared in sterile deionized water, supplemented with penicillin (192 U mL^{-1}), streptomycin (200 μg mL^{-1}), HEPES (25 mM), L-glutamine (3 mM) and 10% of heat-inactivated foetal calf serum (FCS) (pH 7.2). The cells were grown at 310 K in a humidified 5% CO_2 air atmosphere.

MTT assay

Antiproliferative activity of the investigated ligands and complexes was determined using 3-(4,5-dimethyl-2-thiazolyl)-2,5-2H-diphenyltetrazolium bromide (MTT, Sigma-Aldrich) assay.[75] Cells were seeded into 96-well cell culture plates (Thermo Scientific Nunc™), at a cell density of 4000 cells per well (HeLa), 6000 cells per well (A549), 5000 cells per well (MRC-5) and 7000 cells per well (LS174) in 100 μL of culture medium. After 24 h of growth, cells were exposed to the serial dilutions of the tested compounds. The investigated compounds were dissolved in sterile water at a concentration of 10 mM as stock solution (complexes **2** and **4**), 5 mM (complex **1**), or 2 mM (complex **3**), and prior the use diluted with nutrient medium to the desired final concentrations (in range up to 300 μM). Ligands were dissolved in sterile water at a concentration of 10 mM $\mathbf{HL^1}$ and $\mathbf{HL^2}$ and 5 mM $\mathbf{HL^4}$, while ligand $\mathbf{HL^3}$ was dissolved in 1% DMSO at a concentration of 3 mM. Each concentration was tested in triplicates. After incubation periods of 48 h, 20 μL of MTT solution (5 mg mL^{-1} in phosphate buffer solution, pH 7.2) were added to each well. Samples were incubated for 4 h at 310 K, with 5% CO_2 in a humidified atmosphere. Formazan crystals were dissolved in 100 μL of 10% sodium dodecyl sulfate (SDS). Absorbances were recorded after 24 h, on an enzyme-linked immunosorbent assay (ELISA) reader (Thermo Labsystems Multiskan EX 200–240 V), at the wavelength of 570 nm. The IC_{50} value, defined as the concentration of the compound causing 50% cell growth inhibition, was estimated from the dose–response curve.

Results and discussion

These studies examined the effects of attachment of methylpiperazine, morpholine and methylpyrrole-2-carboxylate to the pyridine ring of the parent thiosemicarbazone on the aqueous solubility, lipophilicity, ability to form copper(II) complexes, their thermodynamic stability in aqueous solution, and antiproliferative activity in human cancer cell lines HeLa, A549 and LS174, as well as in nontumorigenic cell line MRC5.

Synthesis and characterization of $\mathbf{HL^1}$–$\mathbf{HL^6}$

The organic hybrids were synthesized in six steps, as shown in Scheme S2.† The first four steps were described in detail previously.[61,76] The key aldehydes were prepared in two steps. First, 2-(chloromethyl)-6-(dimethoxymethyl)pyridine (**D**) was allowed to react with methylpiperazine or morpholine in THF in the presence of triethylamine or with methylpyrrole-2-carboxylate in DMF in the presence of NaH, following a literature procedure,[77] affording compounds **E–G** in 79, 93 and 58% yields, respectively. The aldehydes **H–J** were obtained by hydrolysis of species **E–G** in acidic aqueous solution or in acetone/water 1 : 5 mixture. Finally, condensation reactions of the aldehydes with thiosemicarbazide and/or 4,4-dimethyl-3-thiosemicarbazide afforded the hybrids $\mathbf{HL^1}$–$\mathbf{HL^6}$ in 47–91% yields. One- and two-dimensional ^1H and ^{13}C NMR spectra confirmed the expected structures for $\mathbf{HL^1}$–$\mathbf{HL^6}$ and the presence of *E* and *Z* isomers in DMSO. The *E*/*Z* ratio is 1 : 0.12, 1 : 0.66, 1 : 0.34, 1 : 0.62, 1 : 0.27 and 1 : 0.36 for $\mathbf{HL^1}$–$\mathbf{HL^6}$ respectively, (measured at a concentration of approximately 10 mM). The presence of *E* and *Z* isomers is typical for thiosemicarbazones and our data are in good agreement with those reported for other α-pyridyl-TSCs.[78] The purity of $\mathbf{HL^1}$–$\mathbf{HL^6}$ was further evidenced by elemental analysis. The positive-ion ESI mass spectra of $\mathbf{HL^1}$–$\mathbf{HL^6}$ showed strong peaks at *m*/*z* 293, 321, 280, 308, 317 and 346, respectively, which were assigned to the $[M + H]^+$ ion. The lipo-hydrophilic character of the ligands ($\mathbf{HL^1}$–$\mathbf{HL^5}$) is discussed in the section Solution Chemistry.

Synthesis and characterization of copper(II) complexes

By reaction of $CuCl_2·2H_2O$ with $\mathbf{HL^1}$ and $\mathbf{HL^2}$ in methanol two complexes [CuCl(mPipH-FTSC-H)]Cl·0.1H_2O ((**1** + H)Cl·0.1H_2O) and [CuCl(mPipH-dm-FTSC-H)]Cl·0.9H_2O·0.5CH_3OH ((**2** + H)Cl·0.9H_2O·0.5CH_3OH) were obtained in 74 and 53% yields, respectively. The formulation of both complexes was in accord with X-ray diffraction measurements (*vide infra*) and elemental analyses. Re-crystallization of the first complex from methanol in the presence of a small amount of triethylamine led to crystallization of the complex with deprotonated piperazine moiety, namely [CuCl(mPip-FTSC-H)]·0.15CH_3OH (**1**·0.15CH_3OH), the structure of which was established by single crystal X-ray crystallography. ESI mass spectra of copper(II) complexes with $\mathbf{HL^1}$ and $\mathbf{HL^2}$ showed peaks with *m*/*z* 354 and 382, attributed to $[M - Cl]^+$ ion. The copper(II) complexes [CuCl(Morph-FTSC-H)]·2H_2O·0.2C_2H_5OH (**3**·2H_2O·0.2C_2H_5OH) and [CuCl-(Morph-dm-FTSC-H)]·0.2H_2O·0.6CH_3OH (**4**·0.2H_2O·0.6CH_3OH) were prepared in 88 and 98% yields, by reaction of copper(II)

chloride with HL^3 and HL^4 in ethanol, and methanol, respectively. The composition of both complexes was confirmed by elemental analysis, X-ray diffraction data and ESI mass spectra. The latter showed the presence of peaks at *m*/*z* 341 and 369, assigned to $[M - Cl]^+$ ion. Starting from copper(II) chloride and HL^5 and HL^6 in methanol the complexes [CuCl(mPyrr-FTSC-H)(H_2O)]·0.2H_2O (**5**·0.2H_2O) and [CuCl(mPyrr-dm-FTSC-H)(H_2O)] (**6**) were obtained in 71 and 55% yield, respectively. This was confirmed by elemental analysis and ESI mass spectra. The latter showed the presence of peaks with *m*/*z* 379 and 407, assigned to $[M - Cl - H_2O]^+$ ion. Re-crystallization of [CuCl(mPyrr-FTSC-H)(H_2O)]·0.2H_2O from DMF afforded the complex [CuCl(mPyrr-FTSC-H)(DMF)] (**5**) *via* replacement of coordinated water molecule by DMF, as was confirmed by single crystal X-ray diffraction analysis (see section X-ray Crystallography). Lipo-hydrophilicity data of the copper(II) complexes **1**–**5** are discussed in the section Solution Chemistry.

X-ray crystallography

The results of single crystal X-ray diffraction studies of **1**·0.15CH_3OH, [**2** + H]Cl·2H_2O, **3**·0.5$(C_2H_5)_2O$, **4**·0.93CH_3OH and **5** are shown in Fig. 1–5. The complexes **1**·0.15CH_3OH and **4**·0.93CH_3OH crystallized in the centrosymmetric monoclinic space group $P2_1/n$, while **2**·2H_2O, **3**·0.5$(C_2H_5)_2O$ and **5** crystallized in the centrosymmetric triclinic space group $P\bar{1}$. The piperazine–thiosemicarbazone and morpholine–thiosemicarbazone hybrid ligands HL^1, HL^3 and HL^4 in **1**, **3** and **4** act as tetradentate monodeprotonated ligands coordinating to copper(II) *via* the pyridine nitrogen atom, the azomethine nitrogen, the thiolato S atom and the piperazine or morpholine nitrogen atom, while in [**2** + H]Cl·2H_2O the organic ligand

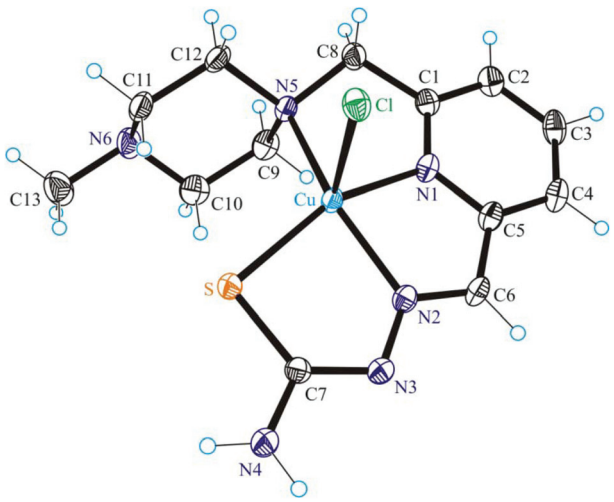

Fig. 1 ORTEP view of **1** with thermal ellipsoids drawn at the 50% probability level. Selected bond distances (Å) and bond angles (°): Cu–N1 1.959(2), Cu–N2 2.011(2), Cu–S 2.2725(7), Cu–N5 2.172(2), Cu–Cl 2.4724(7), N2–N3 1.352(3), C7–S 1.749(3), N1–Cu–N2 79.07(9), N2–Cu–S 83.43(7), N1–Cu–N5 78.60(9), N1–Cu–S 158.26(7), N5–Cu–S 112.56(6), Cl–Cu–N1 96.58(7), Cl–Cu–N2 106.20(7), Cl–Cu–S 100.62(3), Cl–Cu–N5 95.53(6), N2–Cu–N5 150.35(9).

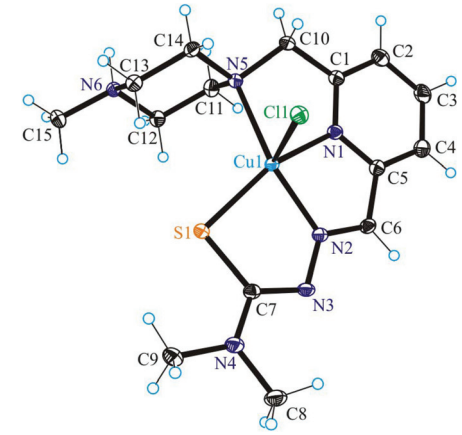

Fig. 2 ORTEP view of $[2 + H]^+$ with thermal ellipsoids drawn at the 50% probability level. Selected bond distances (Å) and bond angles (°): Cu–N1 1.9508(13), Cu–N2 1.9901(13), Cu–S 2.2719(4), Cu–N5 2.2370(13), Cu–Cl 2.4295(4), N2–N3 1.3549(18), C7–S 1.7620(16), N1–Cu–N2 79.91(6), N1–Cu–N5 77.91(2), N2–Cu–S 83.31(4), N5–Cu–S 113.45(4), Cl–Cu–N1 96.25(4), Cl–Cu–N2 109.71(4), Cl–Cu–S 101.600(15), Cl–Cu–N5 89.22(4), N1–Cu–S 158.77(4), N2–Cu–N5 152.23(5).

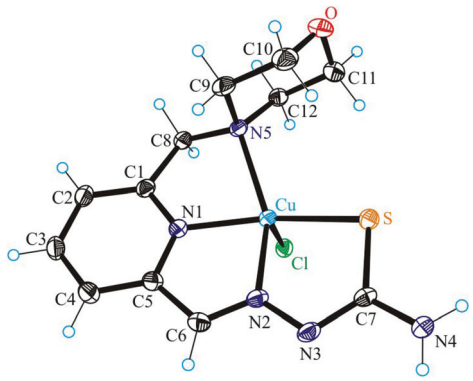

Fig. 3 ORTEP view of **3** with thermal ellipsoids drawn at the 50% probability level. Selected bond distances (Å) and bond angles (°): Cu–N1 1.951(2), Cu–N2 2.004(2), Cu–S 2.2711(7), Cu–N5 2.169(2), Cu–Cl 2.4786(7), N2–N3 1.353(3), C7–S 1.744(2), N1–Cu–N2 79.09(8), N1–Cu–N5 78.88(8), N2–Cu–S 83.37(6), N5–Cu–S 112.30(6), Cl–Cu–N1 96.08(6), Cl–Cu–N2 107.42(6), Cl–Cu–S 101.66(2), Cl–Cu–N5 93.83(6), N1–Cu–S1 158.09(6), N2–Cu–N5 150.76(8).

HL^2 is overall neutral being deprotonated at N3 and protonated at N6. The coordination number of copper(II) is five in complexes **1**–**4** and the coordination polyhedron can be described as a square-pyramid[79] (τ = 0.13, 0.11, 0.12 and 0.10 (0.07 for another crystallographically independent complex), respectively). The apical position is occupied by a chlorido ligand. Three five-membered metallocycles are formed upon binding of the monodeprotonated ligands $(L^1)^-$–$(L^4)^-$ to copper(II). Two of them are essentially planar, while the N1–C1–C8–N5–Cu in **1** and **3**, or N1–C1–C10–N5–Cu in **2** and **4** is markedly distorted. The dihedral angle N1–C1–C8–N5/N1–C1–C10–N5 used here as a measure of the deviation of the chelate

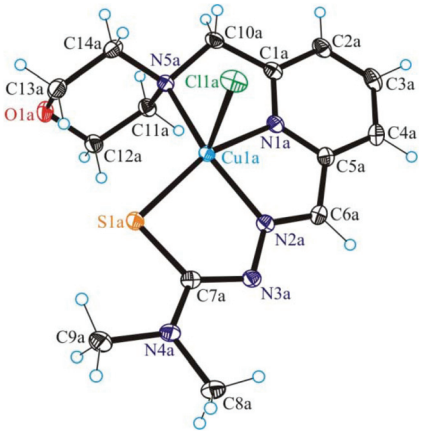

Fig. 4 ORTEP view of one crystallographically independent molecule of **4** with thermal ellipsoids drawn at the 50% probability level. Selected bond distances (Å) and bond angles (°): Cu1a–N1a 1.9388(17), Cu1a–N2a 1.9948(17), Cu1a–S1a 2.2523(6), Cu1a–N5a 2.1406(17), Cu1a–Cl1a 2.5088(6), N2a–N3a 1.358(2), C7a–S1a 1.754(2), N1a–Cu1a–N2a 79.68(7), N1a–Cu1a–N5a 79.90(7), N2a–Cu1a–S1a 83.88(5), N5a–Cu1a–S1a 111.88(5), Cl1a–Cu1a–N1a 91.49(5), Cl1a–Cu1a–N2a 103.19(5), Cl1a–Cu1a–S1a 103.65(2), Cl1a–Cu1a–N5a 93.40(5), N1a–Cu1a–S1a 159.83(5), N2a–Cu1a–N5a 153.91(7). (0.10 and 0.07).

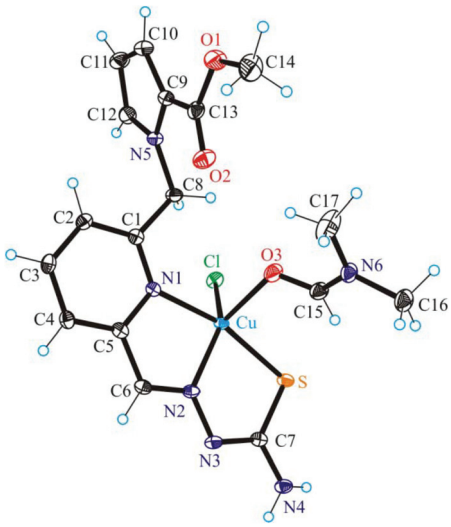

Fig. 5 ORTEP view of **5** with thermal ellipsoids drawn at the 50% probability level. Selected bond distances (Å) and bond angles (°): Cu–N1 2.0912(14), Cu–N2 1.9820(13), Cu–S 2.2785(5), Cu–O3 2.1852(13), Cu–Cl 2.3069(4), N2–N3 1.3641(19), C7–S 1.7387(17), N1–Cu–N2 80.48(6), N2–Cu–S 83.13(4), O3–Cu–S 97.27(2), Cl–Cu–N1 98.97(4), Cl–Cu–N2 137.78(4), Cl–Cu–S 94.701(16), Cl–Cu–O3 107.32(4), N1–Cu–S 163.45(4).

ring from planarity is at −28.1(3) and −28.3(3)° in **1** and **3**, and at −29.62(19) and −22.5(3)° in **2** and **4** (for one of the two crystallographically independent molecules), respectively. This is not surprising if one takes into account the presence of an aliphatic carbon atom (C8/C10) in this chelate ring.

The terminal amine nitrogen N4 of the thiosemicarbazone moiety is involved as a proton donor in hydrogen bonding to the nitrogen atom $N3^{i}$ of a neighboring molecule of **1** forming pairs of molecules as displayed in Fig. S1† and in hydrogen bonding to $Cl1^{ii}$, where i and ii denote the atoms generated by symmetry transformations $-x + 2$, $-y + 1$, $-z + 1$ and $x + 1$, y, z, respectively.

The protonated atom N6 acts as a proton donor to the chloride counterion with $N6\cdots Cl2^{i}$ at 3.0837(14) Å, where i denotes atom positions generated by symmetry transformation $x - 1$, $y + 1$, z, and $N6–H\cdots Cl2^{i}$ 159.5°. Four other hydrogen bonds are formed between the co-crystallized water molecules and the chloride counterion.

Unlike, the hybrid ligand **HL**[5] acts as a tridentate monodeprotonated ligand binding to copper(II) *via* pyridine nitrogen N1, azomethine atom N2 and thiolato atom S. Like in complexes **1**–**4** the coordination number of the copper(II) center in **5** is five, and the coordination geometry shows a slight tendency to square-pyramidal (τ = 0.43), the remaining two places being occupied by the DMF molecule and the chlorido ligand. The pyrrol nitrogen atom N5, due to its sp^2 hybridization remains unbound to copper(II). Note that sp^3-hybridized proline nitrogen atom in proline–thiosemicarbazone conjugates was involved in binding to first-row transition metals and became a chiral center upon coordination.[80]

Solution chemistry: proton dissociation processes of ligands HL[2] and HL[4], lipophilicity of ligands HL[1]–HL[5]

Morph-dm-FTSC (**HL**[4]), which forms the most biologically active copper(II) complex among the studied ligands (*vide infra*), was chosen for the detailed solution equilibrium studies together with its methylpiperazine analogue, mPip-dm-FTSC (**HL**[2]) (Chart 1) for comparison. Deprotonation processes of these ligands were followed in aqueous solution by pH-potentiometric and ^{1}H NMR titrations. Consecutive multiple pH-potentiometric titrations showed that no ligand decomposition occurred in the pH range studied (2.0–11.5) under an argon atmosphere. Morph-dm-FTSC (**HL**[4]) possesses three, while mPip-dm-FTSC (**HL**[2]) four functional groups which, presumably, dissociate. The proton dissociation constants determined by pH-potentiometry are listed in Table 2. The identical *N*-terminally dimethylated α-*N*-pyridyl thiosemicarbazone moiety of the ligands is expected to have a relatively low pK_a value for the $N_{pyridyl}H^+$ and a significantly higher value for the $N_{hydrazinic}H$ functional group based on the proton dissociation constants of structurally similar HCTs, such as 2-formylpyridine N^4,N^4-dimethylthiosemicarbazone (PTSC, pK_1: 3.38 and pK_2: 10.54) or 3-aminopyridine-2-carboxaldehyde N^4, N^4-dimethylthiosemicarbazone (APTSC, pK_1: 4.31 and pK_2: 10.29).[81] Taking into account these data we attributed the pK_2 of Morph-dm-FTSC to the deprotonation of the morpholinium ion. It should also be noted that the assignment of the pK_a values for the methylpiperazine–thiosemicarbazone hybrid is not so straightforward. The proton dissociation steps of the ligands studied were assigned to the different functional

Table 2 Macroscopic and microscopic proton dissociation constants (pK_a) of ligands mPip-dm-FTSC (HL^2) and Morph-dm-FTSC (HL^4) determined by pH-potentiometry and ^{1}H NMR titrations [T = 298 K, I = 0.10 M (KCl)]

	Method		pK_1	pK_2	pK_3	pK_4
mPip-dm-FTSC	pH-metry		1.69 ± 0.02	3.29 ± 0.01	7.88 ± 0.01	10.23 ± 0.01
	^{1}H NMR	Isomer *E*	—	3.59 ± 0.06	7.94 ± 0.01	10.05 ± 0.03
	^{1}H NMR	Isomer *Z*	—	2.24 ± 0.05	7.82 ± 0.01	>11.5
	^{1}H NMR[a]		—	3.33	7.90	10.35
Morph-dm-FTSC	pH-metry		2.27 ± 0.02	5.91 ± 0.01	10.18 ± 0.01	—
	^{1}H NMR	Isomer *E*	2.28 ± 0.01	6.08 ± 0.01	10.14 ± 0.01	—
	^{1}H NMR	Isomer *Z*	<1	5.18 ± 0.01	>11.5	—
	^{1}H NMR[a]		2.21	5.90	10.30	—

[a] Estimated from the summed concentration distribution curves of the *E*/*Z* isomers in Fig. 6B and S4B.

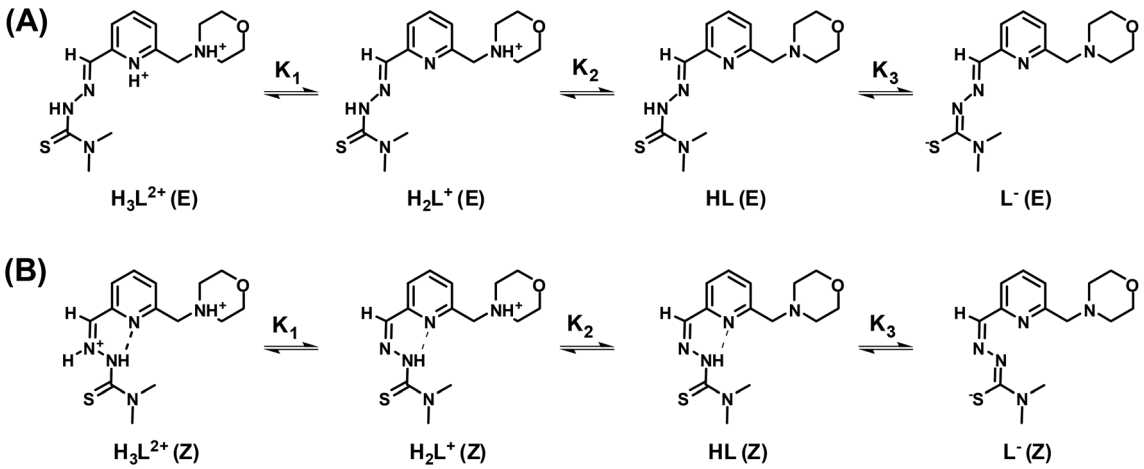

Scheme 1 Deprotonation steps of the H_3L^{2+} form of ligand Morph-dm-FTSC (HL^4) for its *E* (A) and *Z* (B) isomers.

groups by careful analysis of the results of the ^{1}H NMR titrations and are shown in Schemes 1 and S3.†

The pH-dependent ^{1}H NMR spectra of Morph-dm-FTSC (HL^4) (Fig. 7) revealed that most of the proton resonances are fairly sensitive to stepwise proton dissociation processes. In addition, the presence of *Z* and *E* isomers was observed. These were found to be involved in slow interconversion processes with regard to the NMR time scale ($t_{1/2}$(obs) > ~1 ms) in a wide pH-range. Their proton resonances were well-separated in most of the cases. However, the lines tend to broaden at pH < ~4 due to faster isomerization around the $CH^{12}{=}N^1$ double bond. Integrated signals of the different ligand protons belonging to the *E* and *Z* isomers were converted to molar fractions showing the predominant formation of the *E* isomer in the whole pH range, although the ratio of the isomers is undoubtedly changing due to the deprotonation steps (Fig. 6A). The *E* isomer was also found to be the major species in DMSO-d_6 and its molar fraction (0.62) corresponds well to that found for aqueous solution (0.61) between pH ~7 and ~9, where the neutral HL form predominates. Based on the pH-dependence of the ^{1}H NMR signals (Fig. S2†) microscopic proton dissociation constants could be computed for both *Z*

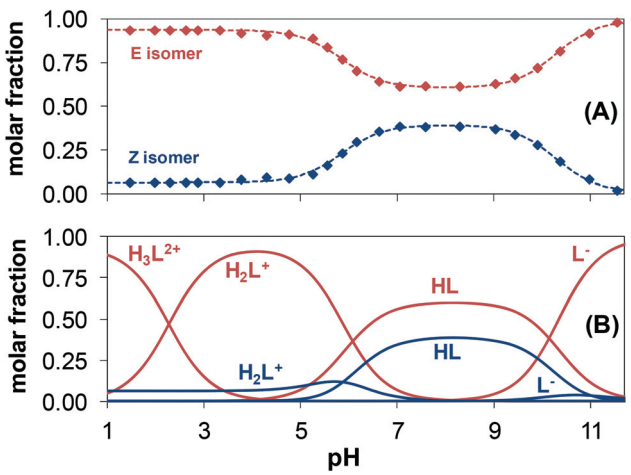

Fig. 6 pH-Dependence of the molar fraction of the *E* (red symbols) and *Z* (blue symbols) isomers of the ligand Morph-dm-FTSC (HL^4) calculated on the basis of the integrated areas of the signals of the various ligand protons (A). Concentration distribution curves for the isomeric ligand species (*E*: labelled in red; *Z*: labelled in blue) calculated with the aid of the microscopic proton dissociation constants (B). [c_L = 1.5 mM; T = 298 K; I = 0.10 M (KCl); 10% D_2O].

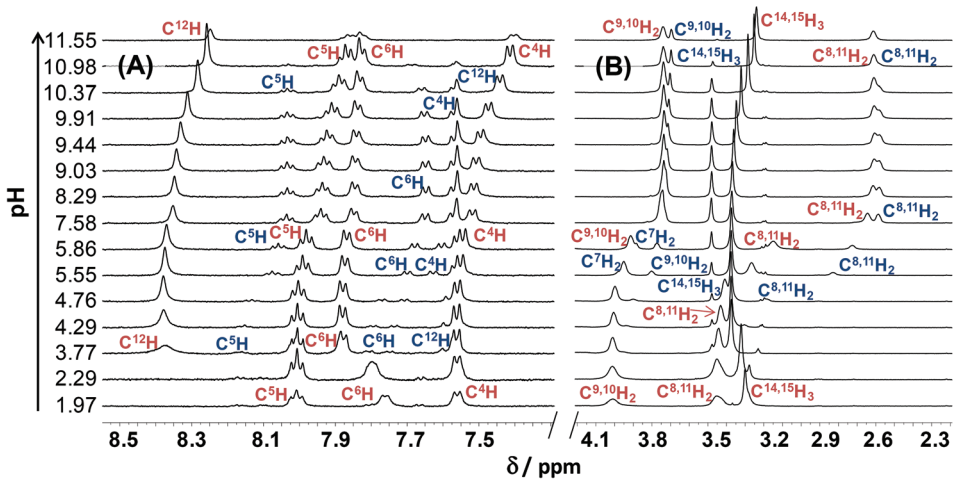

Fig. 7 Low- (A) and high-field (B) regions of the ^{1}H NMR spectra of Morph-dm-FTSC (**HL^4**) at different pH values, red and blue symbols denote the peaks belonging to the protons of the major *E* and minor *Z* isomers, respectively. [c_L = 1.5 mM; *T* = 298 K; *I* = 0.10 M (KCl); 10% D_2O].

and *E* isomers (Table 2). Concentration distribution curves were calculated based on these data providing the macroscopic constants as well (Table 2), which are in good agreement with the results of the pH-potentiometry. The first deprotonation process was accompanied by significant changes of the chemical shifts of the C^6H pyridine ring proton and $C^{14,15}H_3$ terminal methyl protons. The morpholine ($C^{8,11}H_2$, $C^{9,10}H_2$) and C^7H_2 protons were very sensitive to the second deprotonation step, as were also the pyridine ring protons, while the chemical shifts of protons of the thiosemicarbazone moiety ($C^{12}H$, $C^{14,15}H_3$) remain unaltered during the process. In the pH-range where the third proton dissociation occurs the signals of the last mentioned protons were shifted exclusively. These observed changes strongly support the subsequent deprotonation steps of the $N^4_{pyridyl}H^+$, $N^5_{morpholinium}H^+$ and $N^2_{hydrazinic}H$ functional groups of both isomers of Morph-dm-FTSC as indicated in Scheme 1. On the other hand, marked differences are found between the pK_a values of the *Z* and *E* isomers (Table 2). Most probably the hydrogen bond between the pyridyl nitrogen and the $N^2_{hydrazinic}H$ moiety in the H_2L^+, HL forms of the *Z* isomer is responsible for these differences. Namely, it decreases pK_1 of the *Z* isomer *via* stabilization of the conjugate base (H_2L^+) as well as pK_2 due to the diminished π-electron density in the pyridine ring, which results in an easier deprotonation of the $N^5_{morpholinium}H^+$ group. The pK_3 of the *Z* isomer is higher than that of the *E* form, since the dissociation of the $N^2_{hydrazinic}H$ functional group participating in the hydrogen bonding is more difficult.

The pH-dependent ^{1}H NMR spectra of mPip-dm-FTSC (Fig. S3†) and the changes of the chemical shifts of the various protons (Fig. S4†) were analyzed similarly. Data revealed that pK_1 corresponds to the deprotonation of pyridinium nitrogen. However only the macroscopic constant could be determined by pH-potentiometry (Table 2) as the ^{1}H NMR signals were fairly broadened in the pH range where this process takes place and data were not appropriate for calculation. The second deprotonation step is accompanied by significant electronic shielding effects in the case of the pyridine ring protons and a large upfield shift of the C^7H_2 protons. The signals belonging only to the $C^{16}H_3$ methyl protons are sensitive to the third proton dissociation process. These changes strongly indicate that pK_2 and pK_3 can be assigned to the deprotonation of the $N^5_{piperazinium}H^+$ and $N^6_{piperazinium}H^+$ groups, respectively (Scheme S3†). Protons of the thiosemicarbazone moiety were found to be sensitive to the last deprotonation step in which the $N^2_{hydrazinic}H$ releases the proton. Comparing the microscopic constants of the *E* and *Z* isomers of the methylpiperazine–thiosemicarbazone hybrid (Table 2) it can be concluded that the lower pK_2 ($N^5_{piperazinium}H^+$) and higher pK_4 ($N^2_{hydrazinic}H$) values of the *Z* isomer are due to the presence of the hydrogen bond in the H_3L^{2+} and HL forms (see the explanations in the case of Morph-dm-FTSC *vide supra*). At the same time the isomerization has no effect on the pK_3 value since the $N^6_{piperazinium}H^+$ group is quite far from the $CH^{12}{=}N^1$ double bond. The *E* isomer was found to be predominant in the whole pH range studied (Fig. S5†).

It is worth noting that the pK_a values of the $N_{pyridyl}H^+$ functional group of the studied thiosemicarbazone-based hybrids are significantly lower compared to those of ligands PTSC, APTSC[81] due to the electron withdrawing effect of the charged morpholinium and methylpiperazinium moieties.

Both ligands mPip-dm-FTSC (**HL^2**) and Morph-dm-FTSC (**HL^4**) possess intrinsic fluorescence. 3-Dimensional fluorescence spectra recorded in aqueous solution at pH 7.4 (Fig. S6†) reveal their fairly similar excitation (330 nm) and emission maxima (420 nm), although the emission intensity of the morpholine–thiosemicarbazone hybrid is by a factor of 3 higher in comparison to that of **HL^2**.

The lipo-hydrophilic character of the ligands **HL^1**–**HL^5** was studied at pH 7.4 *via* the partitioning between *n*-octanol and

Table 3 Log $D_{7.4}$ values (*n*-octanol/water) for the ligands HL^1–HL^5 and for the copper(II) complexes **1–5** [T = 298 K, pH = 7.40 (10 mM HEPES) and I = 0.10 M (KCl)]

Ligand		log $D_{7.4}$	Complex	log $D_{7.4}$
mPip-FTSC	HL^1	−0.07 ± 0.01	**1**	−1.53 ± 0.09
mPip-dm-FTSC	HL^2	−0.03 ± 0.03	**2**	−0.95 ± 0.10
Morph-FTSC	HL^3	+0.60 ± 0.02	**3**	−1.15 ± 0.09
Morph-dm-FTSC	HL^4	+0.61 ± 0.01	**4**	−0.90 ± 0.09
mPyrr-FTSC	HL^5	>1.8	**5**	>1.8

water. The log $D_{7.4}$ values determined by the analysis of the UV–vis spectra of the aqueous phases before and after separation are listed in Table 3. The results indicate a slightly higher lipophilicity of the terminally dimethylated derivatives (HL^2 and HL^4) compared to that of the corresponding non-methylated ligands (HL^1 and HL^3). Compounds containing the morpholine moiety (HL^3 and HL^4) possess significantly higher log $D_{7.4}$ values compared to those of the methylpiperazine derivatives (HL^1 and HL^2) most probably due to the different protonation states of the ligands at physiological pH. According to the pK_a values of the ligands studied (Table 2) mPip-dm-FTSC (HL^2) is partly protonated (74% H_2L^+, 26% HL), while Morph-dm-FTSC (HL^4) is mainly neutral (97% HL, 3% H_2L^+) at pH 7.4. On the other hand, the methyl ester mPyrr-FTSC (HL^5) is much more lipophilic than the other ligands studied and its high log $D_{7.4}$ value is manifested in a strongly reduced aqueous solubility compared to that of the corresponding proline–thiosemicarbazone conjugates (L- and D-Pro-FTSC: log $D_{7.4}$ < −1.7).[35] It should be also noted that all the ligands studied except mPyrr-FTSC (HL^5) are more hydrophilic than Triapine (log $D_{7.4}$ = +0.85)[69] at physiological pH.

Solution chemistry: complex formation equilibria of copper(II) with ligands HL^2 and HL^4 and lipophilicity of the complexes

The main aim of the studies on complexation reactions of ligands mPip-dm-FTSC (HL^2) and Morph-dm-FTSC (HL^4) with copper(II) was monitoring the stability of the complexes **2** and **4** in aqueous solution especially at physiological pH. The complex formation processes were investigated by the combined use of pH-potentiometric, UV–vis and EPR titrations. The stoichiometries and cumulative stability constants of the complexes furnishing the best fits to the experimental data are listed in Table 4. EPR spectra were recorded at various pH values at 1 : 1 and 1 : 2 metal-to-ligand ratios at room temperature and at 77 K; the fitted experimental and simulated isotropic spectra are depicted in Fig. 8A, B and S7A, B.† The simulation of the EPR spectra resulted in the individual isotropic and anisotropic EPR spectra and parameters of the various species (Fig. 8C, S7C and S8;† Table 5). The EPR measurements at both temperatures revealed the predominant formation of mononuclear mono-ligand complexes in different protonation states. The proton displacement by the metal ion due to complex formation is almost complete already at the starting pH value of the pH-potentiometric titrations (pH ∼ 2) and a negligible amount of free copper(II) was detected by EPR at this pH, indicating the prominently high stability of the complexes formed with both ligands. Therefore, conditional stability constants for $[CuL]^+$, which predominates in a wide pH-range, were determined by competition reactions with EDTA. The displacement of EDTA from the $[Cu(EDTA)]^{2-}$

Table 4 Cumulative (log β), derived and stepwise stability constants of the copper(II) complexes of ligands mPip-dm-FTSC (HL^2) and Morph-dm-FTSC (HL^4) determined by pH-potentiometry, UV–vis and EPR spectroscopy [T = 298 K, I = 0.10 M (KCl)]

		pH-metry	UV–vis	EPR
mPip-dm-FTSC	log β $[CuLH_2]^{3+}$	—	27.5 ± 0.1	27.9 ± 0.1
	log β $[CuLH]^{2+}$	26.53 ± 0.01	26.47 ± 0.01	26.49 ± 0.03
	log β $[CuL]^+$		20.26 ± 0.03[a]	
	log β $[CuLH_{-1}]$	8.4 ± 0.1	8.4 ± 0.1	7.8 ± 0.1
	log β $[CuL_2H]^+$	33.43 ± 0.02	—	33.84 ± 0.06
	log β $[CuL_2]$	—	—	23.71 ± 0.08
	pK_a $[CuLH_2]^{3+}$	—	1.0	1.4
	pK_a $[CuLH]^{2+}$	6.27	6.21	6.23
	pK_a $[CuL]^+$	11.9	11.9	12.5
	log K $[CuL_2]$	—	—	3.45
Morph-dm-FTSC	log β $[CuLH]^{2+}$	20.9 ± 0.1	20.3 ± 0.1	20.7 ± 0.1
	log β $[CuL]^+$		18.86 ± 0.08[a]	
	log β $[CuLH_{-1}]$	7.2 ± 0.1	7.2 ± 0.1	7.0 ± 0.1
	log β $[CuL_2H_3]^{3+}$	40.2 ± 0.1	—	39.90 ± 0.08
	log β $[CuL_2]$	—	—	21.71 ± 0.02
	pK_a $[CuLH]^{2+}$	2.0	1.4	1.8
	pK_a $[CuL]^+$	11.7	11.7	11.9
	log K $[CuL_2]$	—	—	2.85

[a] Determined *via* the EDTA displacement reactions by the ligand HL^2 or HL^4 by UV–vis spectrophotometry. Data for the pK_a values of EDTA (0.9; 1.6; 2.0; 2.66; 6.16; 10.24) and log β of the $[Cu(EDTA)]^{2-}$ complex (18.92) are taken from ref. 61 and conditional stability constants of $[Cu(EDTA)]^{2-}$ calculated for pH 7.4 and 5.6 are 16.06 and 13.61, respectively. Conditional stability constants (log β') of the $[CuL]^+$ species: 16.83 ± 0.03 (HL^2) at pH 7.4 (10 mM HEPES) and 13.79 ± 0.03 (HL^4) at pH 5.6 (10 mM MES). β values of $[CuL]^+$ are calculated as $\beta = \beta' \times \alpha_H$; where $\alpha_H = 1 + \sum\beta\,(H_pL) \times [H^+]^p$.

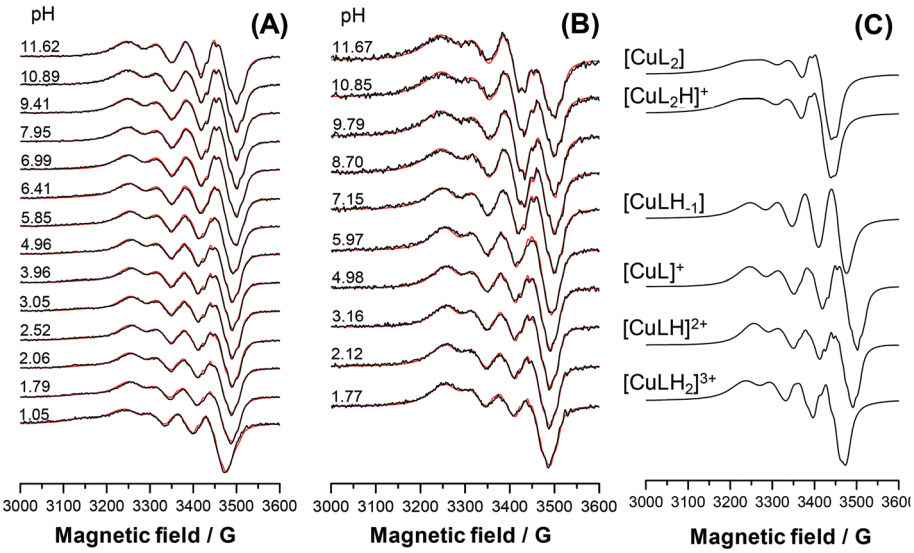

Fig. 8 Experimental (black) and simulated (red) solution EPR spectra recorded for the copper(II)–mPip-dm-FTSC (HL^2) system at 1 : 1 (A) and 1 : 2 (B) metal-to-ligand ratios. Calculated component EPR spectra obtained for the different copper(II)–mPip-dm-FTSC (HL^2) species (C). [c_{ligand} = 1.0 mM; c_{Cu} = 1.0 mM (A) or c_{Cu} = 0.5 mM (B); T = 298 K; I = 0.10 M (KCl)].

Table 5 EPR parameters of the components obtained for the copper(II) complexes of mPip-dm-FTSC (HL^2) and Morph-dm-FTSC (HL^4)

		Isotropic parameters[a]			Anisotropic parameters[b]			Calculated parameters[c]	
		g_o	A_o/G	a_o^N/G	g_x, g_y, g_z	A_x, A_y, A_z[d]/G	a_x^N, a_y^N, a_z^N/G	$g_{o,calc}$	$A_{o,calc}$/G
Morph-dm-FTSC	$[CuLH]^{2+}$	2.1037(2)	68.6(4)	13.8(5) 10.7(7)	2.035, 2.058, 2.216	18.7, 30.4, 155.9	18.5, 13.9, 11.9 12.8, 15.7, 6	2.103	70.7
	$[CuL]^{+}$	2.08856(1)	63.3(1)	17.8(1) 11.9(1) 8.9(2)	2.032, 2.053, 2.176	8.9, 9.8, 160.1	18.2, 9.6, 8.4 10.4, 15.9, 9.8 10.4, 15.9, 9.8	2.087	61.7
	$[CuLH_{-1}]$[e]	2.0953(6)	62.1(8)	9.0(8) 9.0(8)	2.05, 2.07, 2.249	16, 19, 156	8, 17, 8 15, 10, 8	2.121	67.7
	$[CuL_2H_3]^{3+}$	2.0745(5)	85.5(6)	12.3(8) 12.3(8)					
	$[CuL_2]$	2.106(2)	53(2)	17(1) 14(1)					
mPip-dm-FTSC	$[CuLH_2]^{3+}$	2.1026(4)	58.0(5)	17.4(4) 10.3(9)	2.035, 2.059, 2.214	−18.9, 30.4, 155.7	18.4, 14, 12 12, 16.3, 6	2.103	58.5
	$[CuLH]^{2+}$	2.0899(1)	58.3(1)	18.2(1) 11.5(2) 7.8(2)	2.031, 2.055, 2.176	4.4, 8.3, 155.9	16.9, 10.9, 10.9 11.3, 16.8, 9.7 11.3, 16.8, 9.7	2.087	58.3
	$[CuL]^{+}$	2.0894(1)	64.2(1)	17.9(1) 12.1(2) 9.0(3)	2.033, 2.053, 2.177	6.7, 10.9, 159.2	16.7, 9.4, 9 11.7, 16.7, 10 11.7, 16.7, 10	2.088	61.1
	$[CuLH_{-1}]$[e]	2.0959(7)	59(1)	10(1) 10(1)	2.05, 2.07, 2.249	16, 19, 156	8, 17, 8 15, 10, 8	2.121	67.7
	$[CuL_2H]^{+}$	2.1144(6)	54(1)	15(1) 12(2)					
	$[CuL_2]$[e]	2.1118(6)	53(1)	16(1) 12(2)	2.03, 2.05, 2.200	25, −11, 150	17, 10, 10 10, 17, 10	2.093	57

[a] Uncertainties (SD) are shown in parentheses. [b] The experimental errors were ±0.002 for g_x and g_y and ±0.001 for g_z, ± 2 G for A_x and A_y and ±1 G for A_z. [c] Isotropic values calculated *via* the equation $g_o = (g_x + g_y + g_z)/3$, and $A_o[MHz] = (A_x + A_y + A_z)/3$. [d] The signs of the couplings were derived from a comparison of $A_{o,calc}$ with the experimental A_o values. [e] Higher uncertainties of anisotropic parameters were obtained for *minor* species.

complex by the ligands were followed by UV–vis spectrophotometry at pH 7.4 and 5.6, in the case of mPip-dm-FTSC (Fig. S9†) and Morph-dm-FTSC, respectively. Absorbance values recorded at λ > 415 nm were used for calculations of the conditional stability constants ($\log\beta'$) of $[CuL]^+$, the only species contributing to the measured absorbance.

The cumulative stability constants ($\log\beta$) of $[CuL]^+$ were computed (Table 4) taking into account the protonation of the ligands at these pH values, which were kept constant during subsequent data evaluation.

In the case of Morph-dm-FTSC, $[CuL]^+$ predominates between pH ~4 and ~10. This is clearly indicated by the unaltered UV–vis spectra in the wavelength range of both the d–d (Fig. 9) and CT (Fig. S10B†) bands. EPR spectra were also intact in this particular pH range (Fig. S7A†). Based on the EPR parameters of $[CuL]^+$ (Table 5, the superhyperfine couplings to three nitrogen atoms is resolved in the spectra) the coordination of the ligand *via* the (S^-,N^1,N^4,N^5) donor set is the most probable in solution. The rhombic *g*-tensor determined from the anisotropic EPR spectra indicates a strong rhombic distortion which is probably due to the three conjugated five-membered chelate rings formed by the four donor atoms. The single-crystal X-ray crystallography revealed the same binding mode for the ligand in **4** in the solid state (Fig. 4). Upon decreasing the pH complex $[CuL]^+$ becomes protonated and the significant UV–vis (Fig. 9 and S10B†) and EPR (Fig. S7†) spectral changes at pH < ~3 indicate the alteration of the coordination mode. λ_{max} values of both the d–d and CT bands are shifted to the higher wavelengths upon the formation of species $[CuLH]^{2+}$ (578 nm → 690 nm, 406 nm → 410 nm, 302 nm → 323 nm). Most likely, the morpholine nitrogen is protonated and not involved in coordination in $[CuLH]^{2+}$ as indicated by its higher g_0 value compared to that of $[CuL]^+$ (Table 5). On the other hand the deprotonation of $[CuL]^+$ observed at pH > ~10, is accompanied by only minor changes of the UV–vis spectra (see changes at ~256 nm in Fig. S10B†). However, the decreasing ligand field (lower A_0) supports the formation of a mixed hydroxido complex, [CuL(OH)], in which the ligand binds through (S^-,N^1,N^4) donor atoms. A fairly similar deprotonation process of $[CuL]^+$ is characteristic for mPip-dm-FTSC. The formation of $[CuLH_{-1}]$ (=[CuL(OH)]) could be also admitted at the highly basic pH values, although additional changes could be detected in the neutral and acidic pH ranges. Namely, the inflection point of the titration curve recorded at 1 : 1 metal-to-ligand ratio (not shown here) at pH 6.26 strongly suggests an additional (de)protonation process which was not observed in the case of Morph-dm-FTSC. pK_a of species $[CuLH]^{2+}$ was also calculated on the basis of the minor changes of the d–d bands of the UV–vis spectra and the pH-dependent EPR spectra (Fig. 8A). The data obtained by the three different methods are in good agreement (Table 4). The similar g_0 values of $[CuLH]^{2+}$ and $[CuL]^+$ (Table 5) indicate the same coordination mode of mPip-dm-FTSC in these complexes *via* a (S^-,N^1,N^4,N^5) donor atoms both in solution and in the solid state established by X-ray diffraction (Fig. 2), while the ligand field is slightly increased (somewhat higher A_0) due to the deprotonation of $[CuLH]^{2+}$. These results strongly indicate that the process is assigned to the deprotonation of the N^6 of the methylpiperazine moiety which is not involved in the binding to copper(II). The observed UV–vis spectral changes (Fig. S10A†) and EPR parameters (Table 5) at pH < ~3 were found to be similar to those found for the Morph-dm-FTSC system, thus the (S^-,N^1,N^4) coordination is suggested for $[CuLH_2]^{3+}$ in which the methylpiperazine N^5 atom is protonated.

Formation of merely mono-ligand copper(II) complexes for **HL²** and **HL⁴** was expected. However at ligand excess (c_L/c_{Cu} > 2) bis-ligand complexes were detected mainly in the basic pH range. Formation of the neutral bis-ligand complexes $[CuL_2]$ resulted in precipitation which hindered the accurate determination of their stability constants by pH-potentiometry and UV–vis spectrophotometry, although these were estimated by the EPR measurements (Table 4). The EPR data for this kind of complexes represent quite high g_0 and low A_0 values (Table 5) and strong rhombic distortion. The ligands in these complexes coordinate most probably *via* (S^-,N^1,N^4) and ($S_{equatorial}$,N^1_{axial}) donor sets. The stepwise stability constants $\log K$ $[CuL_2]$ are lower by many orders of magnitude than $\log K$ $[CuL]^+$ indicating the non-favored formation of the bis-ligand complexes. Constants for these minor charged bis-ligand complexes such as $[CuL_2H_3]^{3+}$ (Morph-dm-FTSC) and $[CuL_2H]^+$ (mPip-dm-FTSC) could be calculated by pH-potentiometry as well. The former complex displays a well resolved solution EPR spectra with two coordinating N atoms, and large A_0 value which indicate a symmetrical structure with (S^-,N^1) (S^-,N^1) binding mode, while the latter one has a similar coordination pattern as species $[CuL_2]$.

It is worth noting that the isotropic *g* and *A* values calculated by averaging the anisotropic values ($g_{0,calc}$ and $A_{0,calc}$ in Table 5) are in relatively good agreement with the corresponding values measured in solution, indicating that the coordination modes adopted by the ligands in solution are preserved upon freezing.

Representative concentration distribution curves were calculated by using the overall stability constants (average values obtained by the 3 methods) for the copper(II)–mPip-dm-FTSC (**HL²**) and copper(II)–Morph-dm-FTSC (**HL⁴**) systems at 1 : 1 metal-to-ligand ratio to represent the complex formation processes in the pH range studied (Fig. 10). It can be con-

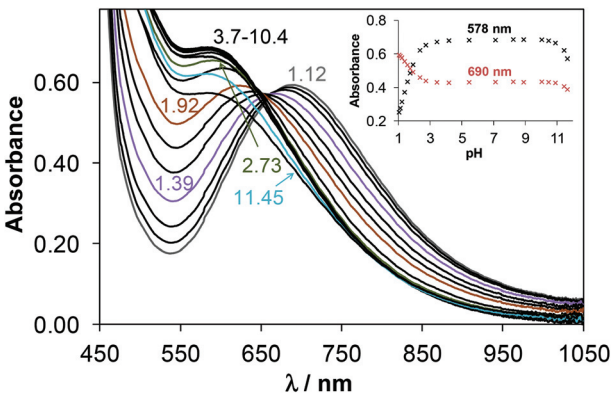

Fig. 9 UV–vis absorbance spectra of **4** recorded in the pH range 1.1–11.7. Inset shows the absorbance values recorded at 578 and 690 nm. [$c_{complex}$ = 2.5 mM; *T* = 298 K; *I* = 0.10 M (KCl); *l* = 1 cm].

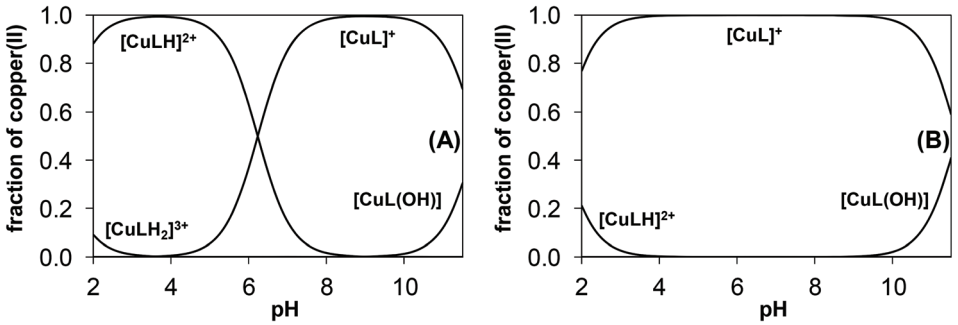

Fig. 10 Concentration distribution curves for the copper(II)–mPip-dm-FTSC (HL^2) (A) and copper(II)–Morph-dm-FTSC (HL^4) (B) systems. [c_L = 1.0 mM; c_{Cu} = 1.0 mM; T = 298 K; I = 0.10 M (KCl)].

cluded that complexes $[CuL]^+$ predominate at physiological pH even at submicromolar concentrations, although 6% of the complex is protonated in the case of mPip-dm-FTSC.

In order to compare the copper(II) binding ability of mPip-dm-FTSC (HL^2) and Morph-dm-FTSC (HL^4) with other thiosemicarbazones pCu values (pCu = –log[Cu(II)]; c_L/c_{Cu} = 10; c_{Cu} = 1 μM) have been computed at physiological pH. The higher pCu value indicates stronger chelating ability. For mPip-dm-FTSC and Morph-dm-FTSC pCu values of 17.6 and 17.0 were obtained, respectively, which are significantly higher than those reported for tridentate HCTs such as Triapine (11.6) at pH 7.4 in 30% (w/w) DMSO/H_2O[82] and are comparable to that of the pentadentate L-Pro-FTSC conjugate (17.5) in pure water.[35]

Log $D_{7.4}$ values were determined for the copper(II) complexes **1–5** and are collected in Table 3 in order to characterize the hydro-lipophilic character of these species. Comparing these values to those of the metal-free ligands it can be concluded that the same lipophilicity trend is obtained. Namely, the terminal dimethylation results in somewhat increased values and complexes of the morpholine–thiosemicarbazone derivatives possess enhanced lipophilic character. Note that the copper(II) complexes are much more hydrophilic than the corresponding ligands since the positively charged $[CuL]^+$ species predominate at physiological pH. Complex **5** is much more lipophilic than the other complexes, although its log $D_{7.4}$ value cannot be determined exactly and compared to that of mPyrr-FTSC (HL^5).

Cytotoxicity in cancer cell lines

The antiproliferative activity of the ligands HL^1–HL^4 and the copper(II) complexes **1–4** was evaluated for 48 h of continuous drug action, using colorimetric MTT assay. The study was performed in three human neoplastic cell lines, namely HeLa (cervical carcinoma), A549 (alveolar basal adenocarcinoma) and LS174 (colon carcinoma), and one human foetal lung fibroblast cell line (MRC-5), which was used as a noncancerous model for the *in vitro* cytotoxicity evaluation. The results for the ligands and their copper(II) complexes are summarized in Table 6 in terms of IC_{50} values with their standard deviations.

Table 6 Results of the MTT assay presented as IC_{50} values obtained after 48 h treatment

IC_{50} [a] [μM] (mean ± SD)				
Compound	HeLa	A549	LS174	MRC5
1	38.3 ± 1.7	62.7 ± 4.7	16.4 ± 4.2	50.6 ± 3.5
2	65.1 ± 5.7	131.3 ± 3.9	17.4 ± 0.2	38.6 ± 5.9
3	63.3 ± 2.7	208.0 ± 0.1	17.5 ± 1.6	132.1 ± 9.2
4	25.5 ± 5.3	42.8 ± 3.7	13.1 ± 2.1	28.3 ± 3.8
HL^1	>300	>300	>300	>300
HL^2	>300	>300	>300	>300
HL^3	>300	>300	>300	>300
HL^4	>300	>300	15.9 ± 0.6	63.2 ± 4.2

[a] The sign > (in front of the maximum value of the concentration) indicates that IC_{50} value is not reached in the examined range of concentrations.

The results revealed that compounds **1–4** exhibited significant antiproliferative activity (IC_{50} < 100 μM) against all cell lines used, with complex **4** showing the highest cytotoxic potential. The most sensitive to the investigated compounds was proved to be the cell line LS174, as indicated by the calculated IC_{50} values varying from 13.1 to 17.5 μM. In contrast, the ligands showed significantly lower activity than the parent 2-formyl- and/or 2-acetylpyridine thiosemicarbazones, except ligand HL^4, which exhibited significant cytotoxic activity against both the MRC5 and LS174 cell lines (63.2 ± 4.2 and 15.9 ± 0.6 μM, respectively).

The metal-free 2-formylpyridine thiosemicarbazone (FTSC) showed high cytotoxicity against human cancer cell lines 41M (ovarian carcinoma), SK-BR-3 (mammary carcinoma), SW480 (colon carcinoma) and HL60 (leukemia) after 96 or 72 h treatment with IC_{50} values of 2.9 ± 0.6, 3.2 ± 0.6, 10.6 ± 0.1 and 3.3 ± 0.5 μM, respectively.[83,84] The effect of substitution of azomethine hydrogen atom by a methyl group is cell line dependent. While there was no change in antiproliferative activity for 2-acetylpyridine thiosemicarbazone (APTSC) in the first two cancer cell lines, a considerable increase was observed against the other two cell lines (IC_{50} = 0.4 ± 0.01 and 0.2 ± 0.02 μM). Terminal N^4-dimethylation of FTSC resulted in a very strong

enhancement of antiproliferative activity reaching IC_{50} values of 0.0040 ± 0.0009 and 0.0098 ± 0.0011 μM in 41M and SK-BR-3 cells after exposure for 96 h.[83] The favorable effect of N^4-dimethylation is also well-documented for other related α-heterocyclic thiosemicarbazones.[31] The coordination of FTSC to copper(II) was reported to increase or decrease the activity depending on the cell type.[85–88] In particular, [Cu(FTSC)Cl_2] revealed an increase of cytotoxicity by a factor of 3 in SW480 cells when compared to that of FTSC, while against HL60 cells the activity of FTSC and the copper(II) complex was very similar.[84] The proline-FTSC hybrids, we synthesized previously,[80] showed a different activity compared to the compounds reported herein. Hybrids that were not methylated at N^4 (L- and D-Pro-FTSC) and their nickel(II), copper(II) and zinc (II) complexes lacked activity (IC_{50} > 300 μM) in both the studied human cancer cell lines HeLa (cervical carcinoma) and A549 (adenocarcinoma), as well as in the non-carcinogenic cell line MRC5 (foetal human fibroblast). The terminally dimethylated hybrid dm-L-Pro-FTSC showed moderate to low anticancer activity with IC_{50} values of 224.6 ± 6.4, 204.3 ± 4.8 and 178.4 ± 1.5 μM in the HeLa, A549 and MRC5 cell lines respectively. Complex formation with copper(II) led to an increased cytotoxicity with IC_{50} values of 93.3 ± 5.5, 176 ± 1.7 and 69.4 ± 4.7 μM in the same cell lines, respectively. Complex formation with zinc(II) or nickel(II) had no favorable effect on the activity. It should be also noted that the copper(II) complex of dm-L-Pro-FTSC showed significant RNR-inhibition activity under reductive conditions at a concentration of 20 μM.[80]

Comparison of IC_{50} values for **3** and **4** indicates that terminal N^4-dimethylation enhances the cytotoxicity in accord with the general trend observed in the literature.[31,83] In contrast, the effect is opposite, although also cell type dependent, if the activity of compounds **1** and **2** is compared. The observed divergent effects of terminal N^4-dimethylation suggest that structural modifications at the pyridine ring (coupling to piperazine and morpholine moieties which increases the denticity of the ligands) play an important role in structure–activity relationships.

Conclusions

The synthesis of new hybrid species as potential ligands for transition metals permitted the study of the effects of the methylpiperazine, morpholine and methylpyrrole-2-carboxylate attachment to the parent 2-formylpyridine thiosemicarbazone on the aqueous solubility, lipophilicity, ability to form copper(II) complexes, their thermodynamic stability and antiproliferative activity in human cancer cell lines HeLa, A549 and LS174, as well as in nontumorigenic cell line MRC5. The hybrid species $\mathbf{HL^5}$ and $\mathbf{HL^6}$ proved to be almost insoluble in water precluding any biological investigations. Attempts to hydrolyze the ester group to –COOH in these two compounds in order to improve the aqueous solubility and ascertain the biological potency of new compounds are undergoing in our laboratory. In contrast, the hybrids $\mathbf{HL^1}$–$\mathbf{HL^4}$ possess excellent water solubility. The solution speciation of copper(II) complexes of $\mathbf{HL^2}$ and $\mathbf{HL^4}$ has been characterized in pure aqueous solution *via* a combined approach using pH-potentiometry, EPR spectroscopy und UV–vis spectrophotometry. The two hybrid compounds were found to act as tetradentate ligands in solution coordinating to copper(II) *via* the (N_{py},N,S^-,N_{hetero}) donor atoms. This binding mode was confirmed by X-ray crystallography in the case of complexes **1–4**. Predominant formation of highly stable $[CuL]^+$ complexes was found at pH 7.4 in aqueous solution and based on the stability constants their decomposition cannot occur even at biologically more relevant micromolar concentrations. The morpholine derivatives $\mathbf{HL^3}$ and $\mathbf{HL^4}$ possess markedly higher $\log D_{7.4}$ values compared to those of the piperazine counterparts $\mathbf{HL^1}$ and $\mathbf{HL^2}$ most probably due to the different protonation states of the hybrid ligands at physiological pH. At the same time they are more hydrophilic than Triapine. Compounds prepared in this work were tested for antiproliferative activity in different human cancer cell lines. Coordination of hybrid ligands $\mathbf{HL^1}$–$\mathbf{HL^4}$ to copper(II) significantly increased the cytotoxicity *in vitro*. While $\mathbf{HL^1}$–$\mathbf{HL^4}$ possess low cytotoxicity with IC_{50} > 300 μM, their copper(II) complexes revealed high antiproliferative activity. The most active compound **4** exhibited IC_{50} values in the range 13.1–42.8 μM in all three human cancer cell lines. Nevertheless the toxicity of the most active complex remains considerably lower when compared to parent 2-formylpyridine and 2-acetylpyridine thiosemicarbazones and their copper(II) complexes which showed IC_{50} values in the nanomolar concentration range and are characterized by very high general toxicity, and, as a consequence have a low therapeutic index. Further experimental work to get insight into the mechanism of action of the prepared copper(II) complexes with hybrid ligands is required to ascertain whether they are really good candidates for further development as potential anticancer drugs.

Acknowledgements

This work was supported by the Hungarian Research Foundation OTKA project PD103905. We are thankful to the Ministry of Science and Technology of Serbia for financial support from grant no. III41026. We thank Prof. M. Galanski for measuring the two-dimensional NMR spectra and Dr Michael Malarek for reading the manuscript and his comments.

Notes and references

1 Y. Yu, D. S. Kalinowski, Z. Kovacevic, A. R. Siafakas, P. J. Jansson, C. Stefani, D. B. Lovejoy, P. C. Sharpe, P. V. Bernhardt and D. R. Richardson, *J. Med. Chem.*, 2009, **52**, 5271–5294.
2 J. S. Casas, M. S. Garcia-Tasende and J. Sordo, *Coord. Chem. Rev.*, 2000, **209**, 197–261.
3 H. Beraldo and D. Gambino, *Mini-Rev. Med. Chem.*, 2004, **4**, 31–39.

4 D. C. Reis, A. A. R. Despaigne, J. G. Da Silva, N. F. Silva, C. F. Vilela, I. C. Mendes, J. A. Takahashi and H. Beraldo, *Molecules*, 2013, **18**, 12645–12662.
5 D. C. Quenelle, K. A. Keith and E. R. Kern, *Antiviral Res.*, 2006, **71**, 24–30.
6 M. A. Salam, M. A. Affan, M. A. Arafat, R. Saha and R. Nasrin, *Heteroat. Chem.*, 2013, **24**, 43–52.
7 A. Molter, J. Rust, C. W. Lehmann, G. Deepa, P. Chiba and F. Mohr, *Dalton Trans.*, 2011, **40**, 9810–9820.
8 S. Arora, S. Agarwal and S. Singhal, *Int. J. Pharm. Pharm. Sci.*, 2014, **6**, 34–41.
9 R. W. Brockman, J. R. Thomson, M. J. Bell and H. E. Skipper, *Cancer Res.*, 1956, **16**, 167–170.
10 S. Wadler, D. Makower, C. Clairmont, P. Lambert, K. Fehn and M. Sznol, *J. Clin. Oncol.*, 2004, **22**, 1553–1563.
11 J. Kolesar, R. C. Brundage, M. Pomplun, D. Alberti, K. Holen, A. Traynor, P. Ivy and G. Wilding, *Cancer Chemother. Pharmacol.*, 2011, **67**, 393–400.
12 C. M. Nutting, H. C. M. L. van, A. B. Miah, S. A. Bhide, J. P. Machiels, J. Buter, C. Kelly, R. D. de and K. J. Harrington, *Annu. Oncol.*, 2009, **20**, 1275–1279.
13 M. J. Mackenzie, D. Saltman, H. Hirte, J. Low, C. Johnson, G. Pond and M. J. Moore, *Invest. New Drugs*, 2007, **25**, 553–558.
14 S. Attia, J. Kolesar, M. R. Mahoney, H. C. Pitot, D. Laheru, J. Heun, W. Huang, J. Eickhoff, C. Erlichman and K. D. Holen, *Invest. New Drugs*, 2008, **26**, 369–379.
15 A. M. Traynor, J.-W. Lee, G. K. Bayer, J. M. Tate, S. P. Thomas, M. Mazurczak, D. L. Graham, J. M. Kolesar and J. H. Schiller, *Invest. New Drugs*, 2010, **28**, 91–97.
16 J. J. Knox, S. J. Hotte, C. Kollmannsberger, E. Winquist, B. Fisher and E. A. Eisenhauer, *Invest. New Drugs*, 2007, **25**, 471–477.
17 F. J. Giles, P. M. Fracasso, H. M. Kantarjian, J. E. Cortes, R. A. Brown, S. Verstovsek, Y. Alvarado, D. A. Thomas, S. Faderl, G. Garcia-Manero, L. P. Wright, T. Samson, A. Cahill, P. Lambert, W. Plunkett, M. Sznol, J. F. DiPersio and V. Gandhi, *Leuk. Res.*, 2003, **27**, 1077–1083.
18 J. E. Karp, F. J. Giles, I. Gojo, L. Morris, J. Greer, B. Johnson, M. Thein, M. Sznol and J. Low, *Leuk. Res.*, 2008, **32**, 71–77.
19 J. F. Zeidner, J. E. Karp, A. L. Blackford, B. D. Smith, I. Gojo, S. D. Gore, M. J. Levis, H. E. Carraway, J. M. Greer, S. P. Ivy, K. W. Pratz and M. A. McDevitt, *Haematologica*, 2014, **99**, 672–678.
20 A. C. Sartorelli, E. C. Moore, M. S. Zedeck and K. C. Agrawal, *Biochemistry*, 1970, **9**, 4492–4498.
21 F. A. French, E. J. Blanz Jr., S. C. Shaddix and R. W. Brockman, *J. Med. Chem.*, 1974, **17**, 172–181.
22 M. Kolberg, K. R. Strand, P. Graff and K. Kristoffer Andersson, *Biochim. Biophys. Acta, Proteins Proteomics*, 2004, **1699**, 1–34.
23 J. L. Nitiss, *Nat. Rev. Cancer*, 2009, **9**, 327–337.
24 A. J. Schoeffler and J. M. Berger, *Q. Rev. Biophys.*, 2008, **41**, 41–101.
25 J. Easmon, G. Puerstinger, G. Heinisch, T. Roth, H. H. Fiebig, W. Holzer, W. Jaeger, M. Jenny and J. Hofmann, *J. Med. Chem.*, 2001, **44**, 2164–2171.
26 L. Wei, J. Easmon, R. K. Nagi, B. D. Muegge, L. A. Meyer and J. S. Lewis, *J. Nucl. Med.*, 2006, **47**, 2034–2041.
27 A. M. Merlot, D. S. Kalinowski and D. R. Richardson, *Antioxid. Redox Signaling*, 2013, **18**, 973–1006.
28 L. Zhu, B. Zhou, X. Chen, H. Jiang, J. Shao and Y. Yun, *Biochem. Pharmacol.*, 2009, **78**, 1178–1185.
29 A. Popovic-Bijelic, C. R. Kowol, M. E. S. Lind, J. Luo, F. Himo, E. A. Enyedy, V. B. Arion and A. Graeslund, *J. Inorg. Biochem.*, 2011, **105**, 1422–1431.
30 Y. Aye, M. J. C. Long and J. Stubbe, *J. Biol. Chem.*, 2012, **287**, 35768–35778.
31 H. Huang, Q. Chen, K. Xin, L. Meng, L. Lin, X. Wang, C. Zhu, Y. Wang, Z. Chen, M. Li, H. Jiang, K. Chen, J. Ding and H. Liu, *J. Med. Chem.*, 2010, **53**, 3048–3064.
32 B. M. Zeglis, V. Divilov and J. S. Lewis, *J. Med. Chem.*, 2011, **54**, 2391–2398.
33 C. R. Kowol, R. Eichinger, M. A. Jakupec, M. Galanski, V. B. Arion and B. K. Keppler, *J. Inorg. Biochem.*, 2007, **101**, 1946–1957.
34 C. R. Kowol, R. Berger, R. Eichinger, A. Roller, M. A. Jakupec, P. P. Schmidt, V. B. Arion and B. K. Keppler, *J. Med. Chem.*, 2007, **50**, 1254–1265.
35 F. Bacher, E. A. Enyedy, N. V. Nagy, A. Rockenbauer, G. M. Bognar, R. Trondl, M. S. Novak, E. Klapproth, T. Kiss and V. B. Arion, *Inorg. Chem.*, 2013, **52**, 8895–8908.
36 O. A. Troshina, P. A. Troshin, A. S. Peregudov, V. I. Kozlovski and R. N. Lyubovskaya, *Chem. – Eur. J.*, 2006, **12**, 5569–5577.
37 C. Antonello, E. Uriarte, M. Palumbo, S. Valisena, C. Parolin and G. Palu, *Eur. J. Med. Chem.*, 1993, **28**, 291–296.
38 T. W. Moore, K. Sana, D. Yan, P. Thepchatri, J. M. Ndungu, M. T. Saindane, M. A. Lockwood, M. G. Natchus, D. C. Liotta, R. K. Plemper, J. P. Snyder and A. Sun, *Beilstein J. Org. Chem.*, 2013, **9**, 197–203.
39 L. K. Filak, D. S. Kalinowski, T. J. Bauer, D. R. Richardson and V. B. Arion, *Inorg. Chem.*, 2014, **53**, 6934–6943.
40 N. Ae and Y. Fujiwara, *US Pat.*, US20110263847A1, 2011.
41 Y. Kakiya and M. Oda, *WO Pat.*, WO2005009999A1, 2005.
42 T. Ochi, M. Sakamoto, A. Minamida, K. Suzuki, T. Ueda, T. Une, H. Toda, K. Matsumoto and Y. Terauchi, *Bioorg. Med. Chem. Lett.*, 2005, **15**, 1055–1059.
43 B.-C. Chen, R. Droghini, J. Lajeunesse, J. D. Dimarco, M. Galella and C. Ramakrishnan, *WO Pat.*, WO2005077945A2, 2005.
44 R. Kharb, K. Bansal and A. K. Sharma, *Pharm. Chem.*, 2012, **4**, 2470–2488.
45 J. Faist, W. Seebacher, R. Saf, R. Brun, M. Kaiser and R. Weis, *Eur. J. Med. Chem.*, 2012, **47**, 510–519.
46 K. Kulig, J. Sapa, D. Maciag, B. Filipek and B. Malawska, *Arch. Pharm.*, 2007, **340**, 466–475.
47 J. M. Nelson, T. M. Chiller, J. H. Powers and F. J. Angulo, *Clin. Infect. Dis.*, 2007, **44**, 977–980.
48 J. M. Burka, K. S. Bower, R. C. Vanroekel, R. D. Stutzman, C. P. Kuzmowych and R. S. Howard, *Am. J. Ophthalmol.*, 2005, **140**, 83–87.

49 D. S. Schiller and H. B. Fung, *Clin. Ther.*, 2007, **29**, 1862–1886.
50 B. Macias, M. V. Villa, I. Rubio, A. Castineiras and J. Borras, *J. Inorg. Biochem.*, 2001, **84**, 163–170.
51 P. Drevensek, J. Kosmrlj, G. Giester, T. Skauge, E. Sletten, K. Sepcic and I. Turel, *J. Inorg. Biochem.*, 2006, **100**, 1755–1763.
52 I. Turel, J. Kljun, F. Perdih, E. Morozova, V. Bakulev, N. Kasyanenko, J. A. W. Byl and N. Osheroff, *Inorg. Chem.*, 2010, **49**, 10750–10752.
53 A. Tarushi, E. Polatoglou, J. Kljun, I. Turel, G. Psomas and D. P. Kessissoglou, *Dalton Trans.*, 2011, **40**, 9461–9473.
54 R. Zia ur, N. Muhammad, S. Ali, I. S. Butler and A. Meetsma, *Inorg. Chim. Acta*, 2011, **376**, 381–388.
55 Q.-P. Shi, Z.-H. Shi, N.-G. Li, Y.-P. Tang, T. Hao, W. Zhang, M.-Z. Shen, Z.-X. Dong, P.-X. Zhang, J.-P. Yang and J.-A. Duan, *Lett. Org. Chem.*, 2014, **11**, 590–595.
56 C. Cano, K. Saravanan, C. Bailey, J. Bardos, N. J. Curtin, M. Frigerio, B. T. Golding, I. R. Hardcastle, M. G. Hummersone, K. A. Menear, D. R. Newell, C. J. Richardson, K. Shea, G. C. M. Smith, P. Thommes, A. Ting and R. J. Griffin, *J. Med. Chem.*, 2013, **56**, 6386–6401.
57 C. Cano, O. R. Barbeau, C. Bailey, X.-L. Cockcroft, N. J. Curtin, H. Duggan, M. Frigerio, B. T. Golding, I. R. Hardcastle, M. G. Hummersone, C. Knights, K. A. Menear, D. R. Newell, C. J. Richardson, G. C. M. Smith, B. Spittle and R. J. Griffin, *J. Med. Chem.*, 2010, **53**, 8498–8507.
58 K. B. Kim and C. M. Crews, *Nat. Prod. Rep.*, 2013, **30**, 600–604.
59 J. Wang, M. Sanchez-Rosello, J. L. Acena, C. del Pozo, A. E. Sorochinsky, S. Fustero, V. A. Soloshonok and H. Liu, *Chem. Rev.*, 2014, **114**, 2432–2506.
60 K. C. Agrawal, B. A. Booth, S. M. DeNuzzo and A. C. Sartorelli, *J. Med. Chem.*, 1976, **19**, 1209–1214.
61 G. Paolucci, A. Zanella, M. Bortoluzzi, S. Sostero, P. Longo and M. Napoli, *J. Mol. Catal. A: Chem.*, 2007, **272**, 258–264.
62 D. B. G. Williams and M. Lawton, *J. Org. Chem.*, 2010, **75**, 8351–8354.
63 G. Gran, *Acta Chem. Scand.*, 1950, **4**, 559–577.
64 H. M. N. H. Irving, M. G. Miles and L. D. Pettit, *Anal. Chim. Acta*, 1967, **38**, 475–488.
65 SCQuery, *The IUPAC Stability Constants Database, Academic Software (Version 5.5)*.
66 P. Gans, A. Sabatini and A. Vacca, *Talanta*, 1996, **43**, 1739–1753.
67 L. Zékány and I. Nagypál, in *Computational Methods for the Determination of Stability Constants*, ed. D. L. Leggett, Plenum Press, New York, 1985, pp. 291–353.
68 E. A. Enyedy, E. Zsigo, N. V. Nagy, C. R. Kowol, A. Roller, B. K. Keppler and T. Kiss, *Eur. J. Inorg. Chem.*, 2012, 4036–4047.
69 M. N. M. Milunovic, E. A. Enyedy, N. V. Nagy, T. Kiss, R. Trondl, M. A. Jakupec, B. K. Keppler, R. Krachler, G. Novitchi and V. B. Arion, *Inorg. Chem.*, 2012, **51**, 9309–9321.
70 A. Rockenbauer, T. Szabo-Planka, Z. Arkosi and L. Korecz, *J. Am. Chem. Soc.*, 2001, **123**, 7646–7654.
71 A. Rockenbauer and L. Korecz, *Appl. Magn. Reson.*, 1996, **10**, 29–43.
72 SAINT-Plus, *version 7.06a and APEX2*, Bruker-Nonius AXS Inc., Madison, WI, 2004.
73 G. M. Sheldrick, *Acta Crystallogr., Sect. A: Found. Crystallogr.*, 2008, **64**, 112–122.
74 L. J. Farrugia, *J. Appl. Crystallogr.*, 1997, **30**, 565.
75 R. Supino, in *In Vitro Toxicity Testing Protocols*, ed. S. O'Hare and C. Atterwill, Humana Press, 1995, vol. 43, ch. 16, pp. 137–149.
76 A. Ojida, T. Sakamoto, M.-a. Inoue, S.-h. Fujishima, G. Lippens and I. Hamachi, *J. Am. Chem. Soc.*, 2009, **131**, 6543–6548.
77 T. Watanabe, A. Kobayashi, M. Nishiura, H. Takahashi, T. Usui, I. Kamiyama, N. Mochizuki, K. Noritake, Y. Yokoyama and Y. Murakami, *Chem. Pharm. Bull.*, 1991, **39**, 1152–1156.
78 M. M. B. Pessoa, G. F. S. Andrade, V. R. Paoli Monteiro and M. L. A. Temperini, *Polyhedron*, 2001, **20**, 3133–3141.
79 A. W. Addison, T. N. Rao, J. Reedijk, J. Van Rijn and G. C. Verschoor, *J. Chem. Soc., Dalton Trans.*, 1984, 1349–1356.
80 F. Bacher, O. Doemoetoer, M. Kaltenbrunner, M. Mojovic, A. Popovic-Bijelic, A. Graeslund, A. Ozarowski, L. Filipovic, S. Radulovic, E. A. Enyedy and V. B. Arion, *Inorg. Chem.*, 2014, **53**, 12595–12609.
81 E. A. Enyedy, M. F. Primik, C. R. Kowol, V. B. Arion, T. Kiss and B. K. Keppler, *Dalton Trans.*, 2011, **40**, 5895–5905.
82 E. A. Enyedy, N. V. Nagy, E. Zsigo, C. R. Kowol, V. B. Arion, B. K. Keppler and T. Kiss, *Eur. J. Inorg. Chem.*, 2010, 1717–1728.
83 C. R. Kowol, R. Trondl, P. Heffeter, V. B. Arion, M. A. Jakupec, A. Roller, M. Galanski, W. Berger and B. K. Keppler, *J. Med. Chem.*, 2009, **52**, 5032–5043.
84 C. R. Kowol, P. Heffeter, W. Miklos, L. Gille, R. Trondl, L. Cappellacci, W. Berger and B. K. Keppler, *JBIC, J. Biol. Inorg. Chem.*, 2012, **17**, 409–423.
85 L. A. Saryan, E. Ankel, C. Krishnamurti, D. H. Petering and H. Elford, *J. Med. Chem.*, 1979, **22**, 1218–1221.
86 E. W. Ainscough, A. M. Brodie, W. A. Denny, G. J. Finlay and J. D. Ranford, *J. Inorg. Biochem.*, 1998, **70**, 175–185.
87 J. Garcia-Tojal, A. Garcia-Orad, A. Alvarez Diaz, J. L. Serra, M. K. Urtiaga, M. I. Arriortua and T. Rojo, *J. Inorg. Biochem.*, 2001, **84**, 271–278.
88 G. Pelosi, *Open Crystallogr. J.*, 2010, **3**, 16–28.